THIS REPORT HAS BEEN DELIMITED
AND CLEARED FOR PUBLIC RELEASE
UNDER DOD DIRECTIVE 5200.20 AND
NO RESTRICTIONS ARE IMPOSED UPON
ITS USE AND DISCLOSURE.

DISTRIBUTION STATEMENT A

APPROVED FOR PUBLIC RELEASE;
DISTRIBUTION UNLIMITED.

SECURITY MARKING

The classified or limited status of this report applies to each page, unless otherwise marked.
Separate page printouts MUST be marked accordingly.

THIS DOCUMENT CONTAINS INFORMATION AFFECTING THE NATIONAL DEFENSE OF THE UNITED STATES WITHIN THE MEANING OF THE ESPIONAGE LAWS, TITLE 18, U.S.C., SECTIONS 793 AND 794. THE TRANSMISSION OR THE REVELATION OF ITS CONTENTS IN ANY MANNER TO AN UNAUTHORIZED PERSON IS PROHIBITED BY LAW.

NOTICE: When government or other drawings, specifications or other data are used for any purpose other than in connection with a definitely related government procurement operation, the U. S. Government thereby incurs no responsibility, nor any obligation whatsoever; and the fact that the Government may have formulated, furnished, or in any way supplied the said drawings, specifications, or other data is not to be regarded by implication or otherwise as in any manner licensing the holder or any other person or corporation, or conveying any rights or permission to manufacture, use or sell any patented invention that may in any way be related thereto.

474352

BRL R 1295

BRL

AD

REPORT NO. 1295

THE EFFECT OF VARIOUS BOATTAIL SHAPES ON BASE PRESSURE AND OTHER AERODYNAMIC CHARACTERISTICS OF A 7-CALIBER LONG BODY OF REVOLUTION AT M = 1.70

by

B. G. Karpov

DDC
DEC 9 1965
TISIA E

AUGUST 1965

U. S. ARMY MATERIEL COMMAND
BALLISTIC RESEARCH LABORATORIES
ABERDEEN PROVING GROUND, MARYLAND

Destroy this report when it is no longer needed.
Do not return it to the originator.

DDC AVAILABILITY NOTICE

Qualified requesters may obtain copies of this report from DDC.

Release or announcement to the public is not authorized

The findings in this report are not to be construed as an official Department of the Army position, unless so designated by other authorized documents.

B A L L I S T I C R E S E A R C H L A B O R A T O R I E S

REPORT NO. 1295

AUGUST 1965

THE EFFECT OF VARIOUS BOATTAIL SHAPES ON BASE PRESSURE AND OTHER AERODYNAMIC CHARACTERISTICS OF A 7-CALIBER LONG BODY OF REVOLUTION AT M = 1.70

B. G. Karpov

Exterior Ballistics Laboratory

RDT&E Project No. 1P014501A33D

A B E R D E E N P R O V I N G G R O U N D, M A R Y L A N D

PREVIOUS PAGE WAS BLANK, THEREFORE NOT FILMED

B A L L I S T I C R E S E A R C H L A B O R A T O R I E S

REPORT NO. 1295

BGKarpov/blw
Aberdeen Proving Ground, Md.
August 1965

THE EFFECT OF VARIOUS BOATTAIL SHAPES ON BASE PRESSURE AND OTHER AERODYNAMIC CHARACTERISTICS OF A 7-CALIBER LONG BODY OF REVOLUTION AT M = 1.70

ABSTRACT

Models, 7 calibers long, with a variety of conical, ogival (convex) and concave boattails were free-flight tested at M = 1.70, for drag and other aerodynamic characteristics. The total drag decreases monotonically for boattails longer than 0.5 calibers. For shorter boattails, the drag is higher than that of the square based body. For boattail lengths between 0.5 and 1.5 calibers, conical boattails have lower drag than either the ogival or concave configurations.

The base pressure decreases with boattail length but increases with the boattail angle at the base.

Among other aerodynamic characteristics, the boattailing appears to cause the most significant change in the Magnus torque coefficient. For certain boattails, this change may be sufficiently large to make the configuration dynamically unstable.

PREVIOUS PAGE WAS BLANK, THEREFORE NOT FILMED

TABLE OF CONTENTS

PREVIOUS PAGE WAS BLANK, THEREFORE NOT FILMED

LIST OF SYMBOLS

C_{D_o}	Total drag coefficient at zero lift
$C_{D_{\overline{\delta^2}}}$	Yaw drag coefficient, per sq. radian, defined by Equation (1)
$\overline{\delta^2}$	Mean square yaw, sq. radians
C_{DH}	Head drag coefficient
C_{DBT}	Boattail drag coefficient
C_{DSF}	Skin friction drag coefficient
C_{DB}	Base drag coefficient
p_b	Bass pressure
p_1	Free stream static pressure
p'	Local static pressure
p_t	Total pressure
C_{L_α}	Lift coefficient
$C_{M_q} + C_{M_{\dot{\alpha}}}$	Damping moment coefficient
$C_{M_{p\alpha}}$	Magnus torque coefficient
C_{ℓ_p}	Axial torque coefficient

1. INTRODUCTION

The data contained herein were obtained some twelve years ago but, for one reason or another, have never been published. The program was designed to study the effect of various boattail configurations on drag and base pressure. Its inauguration was stimulated by a memorandum written by J. Sternberg to R. H. Kent, then Chief of the Exterior Ballistics Laboratory, suggesting a semi-empirical method for estimating base pressures of boattailed bodies of revolution in supersonic flight. Because of its historical interest, this memorandum is reproduced in toto in the appendix.

It was well known that, in general, boattailing of a spin-stabilized projectile reduced its drag. At subsonic speeds the drag decreases monotonically with increasing boattail angle, at least for a reasonable range of boattail lengths and angles, until separation of the flow off the boattail takes place. At supersonic speeds, for conical boattails, there is an optimum boattail angle, of about 6 to 7 degrees which appears to persist to relatively high Mach numbers[1*].

The question of whether other than a conical boattail might be more effective in reducing drag is intimately connected with the effect of boattail shape on base pressure. Thus, to test this and also Sternberg's suggestion, this program was fired. However, unavoidable delays prevented its execution in a reasonable time. Meanwhile, other investigators, notably Chapman, had developed reliable methods for estimating the base pressure of bodies of revolution in supersonic flight. Thus, interest in the original purpose of the program waned and pressure of other work effectively terminated this effort. Nevertheless, while interest in the base pressure per se might have decreased, analysis of the firing data uncovered interesting effects of boattailing on other aerodynamic coefficients and in particular, on the dynamic stability. Therefore, in view of recent enhancement of interest in long projectiles, the publication of these results may still serve a useful purpose.

Superscript numbers denote references found on page 40.

2. PROJECTILE DESIGN

The solid aluminum projectile was a body of revolution 7 calibers in overall length. The head was 2.5 calibers long and consisted of a conical nose one caliber in length of 16° 4.5′ semi-apex angle which was joined by a circular arc to the body. To facilitate theoretical computations of pressure distribution over the body, the circular arc was tangent both to the cone and to the cylindrical body. A schematic drawing of a model is shown in Figure 1.

2.1 Boattails

Three types of boattails were used: conical, ogival (or convex), and concave. Conical boattails were of two types: (1) the length of the boattail was kept constant at $\ell = 0.69$ calibers and the angle varied in increments of two degrees from 0° to 12°, Plate I, (2) the base diameter was kept constant at $d_B = 0.708$ calibers, and the angle was varied by varying the length of the boattail. Ogival and concave boattails also had the same base diameter of 0.708 calibers. The ogival boattails were tangent to the cylindrical body and their angles were also varied by changing their lengths. The angle at the base of such a boattail is always twice the corresponding angle of a conical boattail of equal length. Concave boattails approached the base at zero angle, their breakaway angle was equal to that of the ogival boattail of the same length.

All models were fired at M = 1.70 from 20mm gun tube having a twist of rifling of one turn in ten calibers of travel. All were gyroscopically stable in flight. The Reynolds number, based on overall length. and free stream conditions, was 5.36×10^{6}. The aerodynamic range where these firings were done is fully described in Reference 2, and the method of analysis of the observed motion is given in Reference 3. One model, in flight, is shown in Plate II.

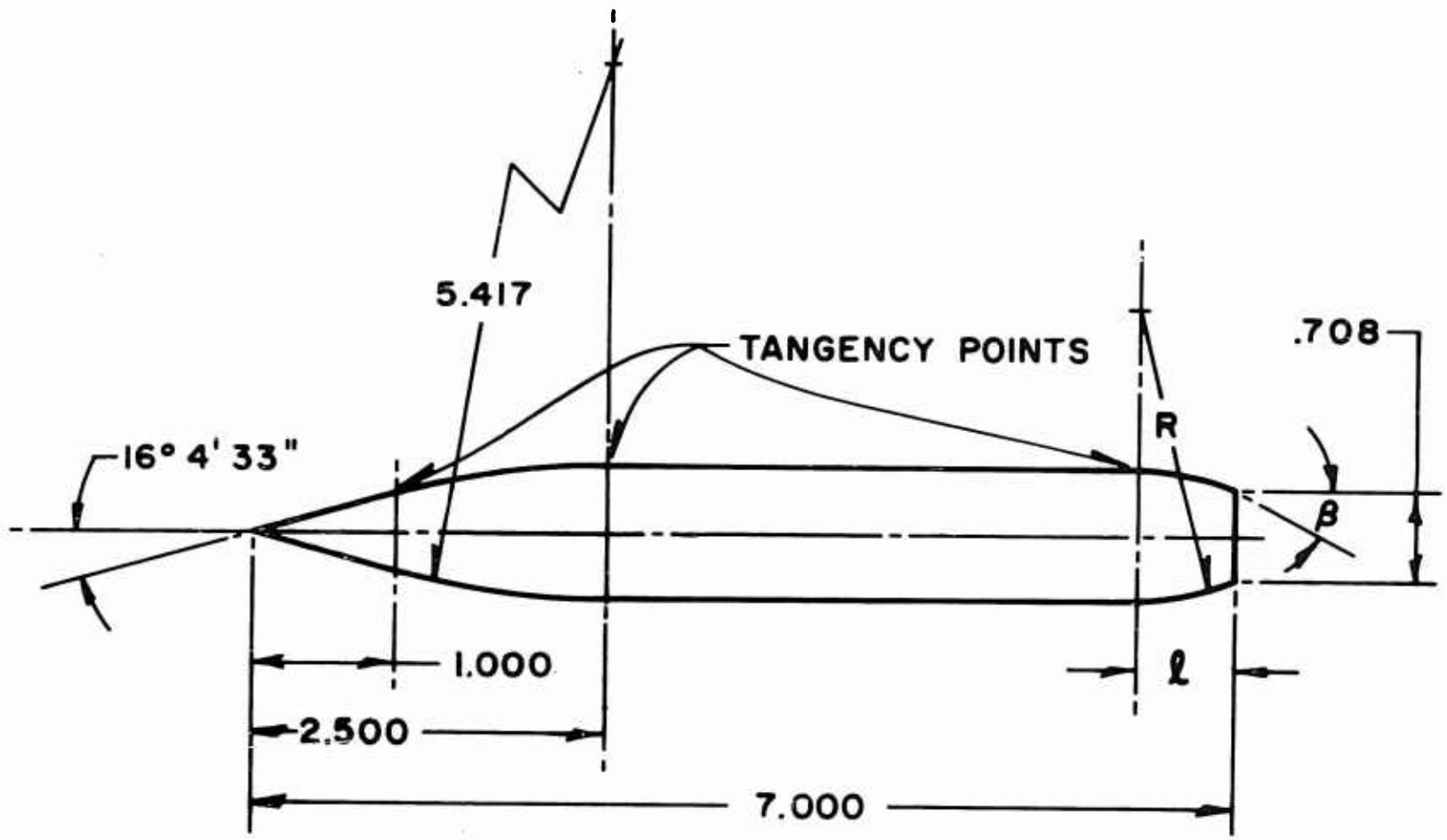

ALL DIMENSIONS ARE IN CALIBERS

FIG. 1

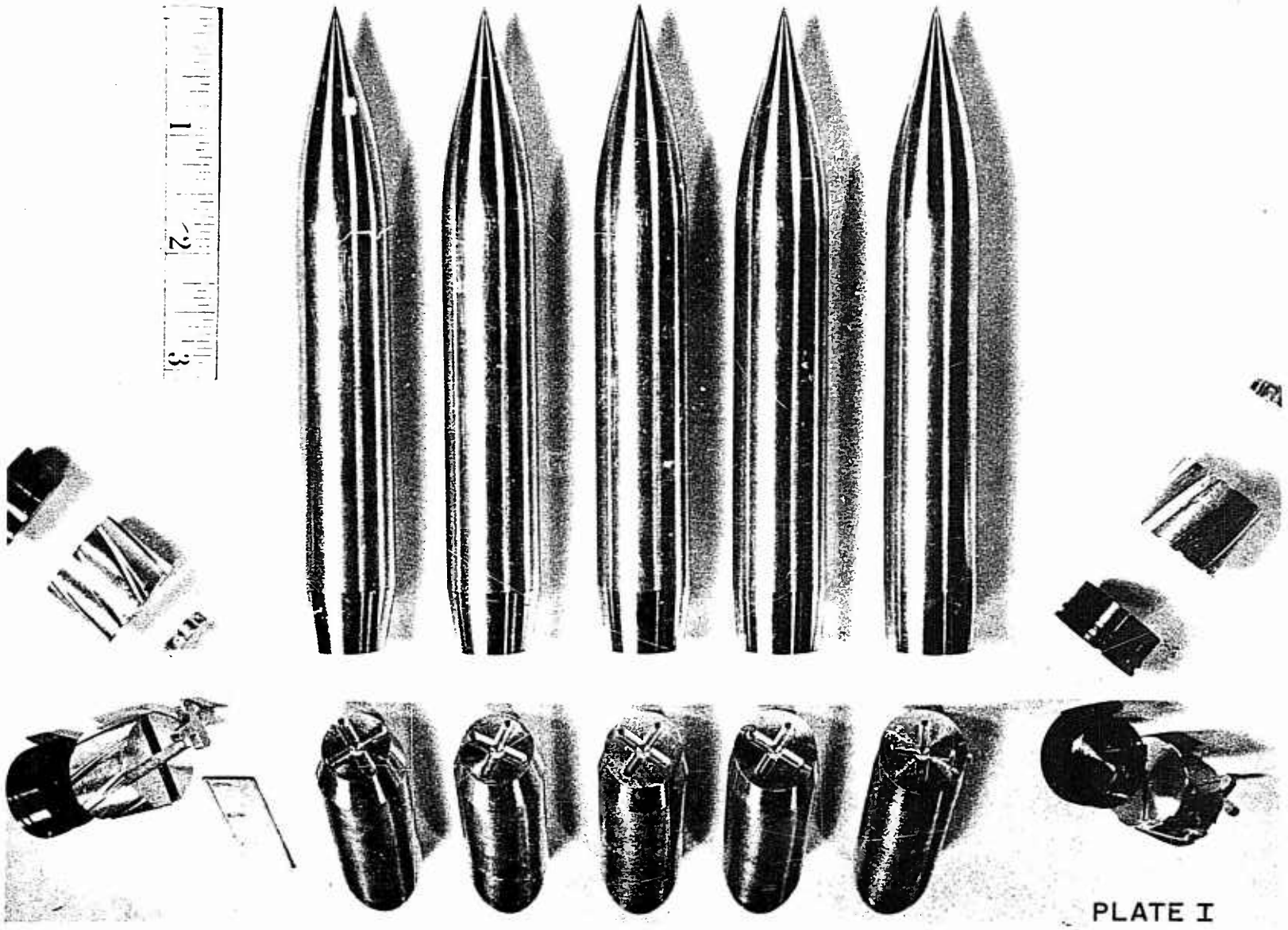

PLATE I

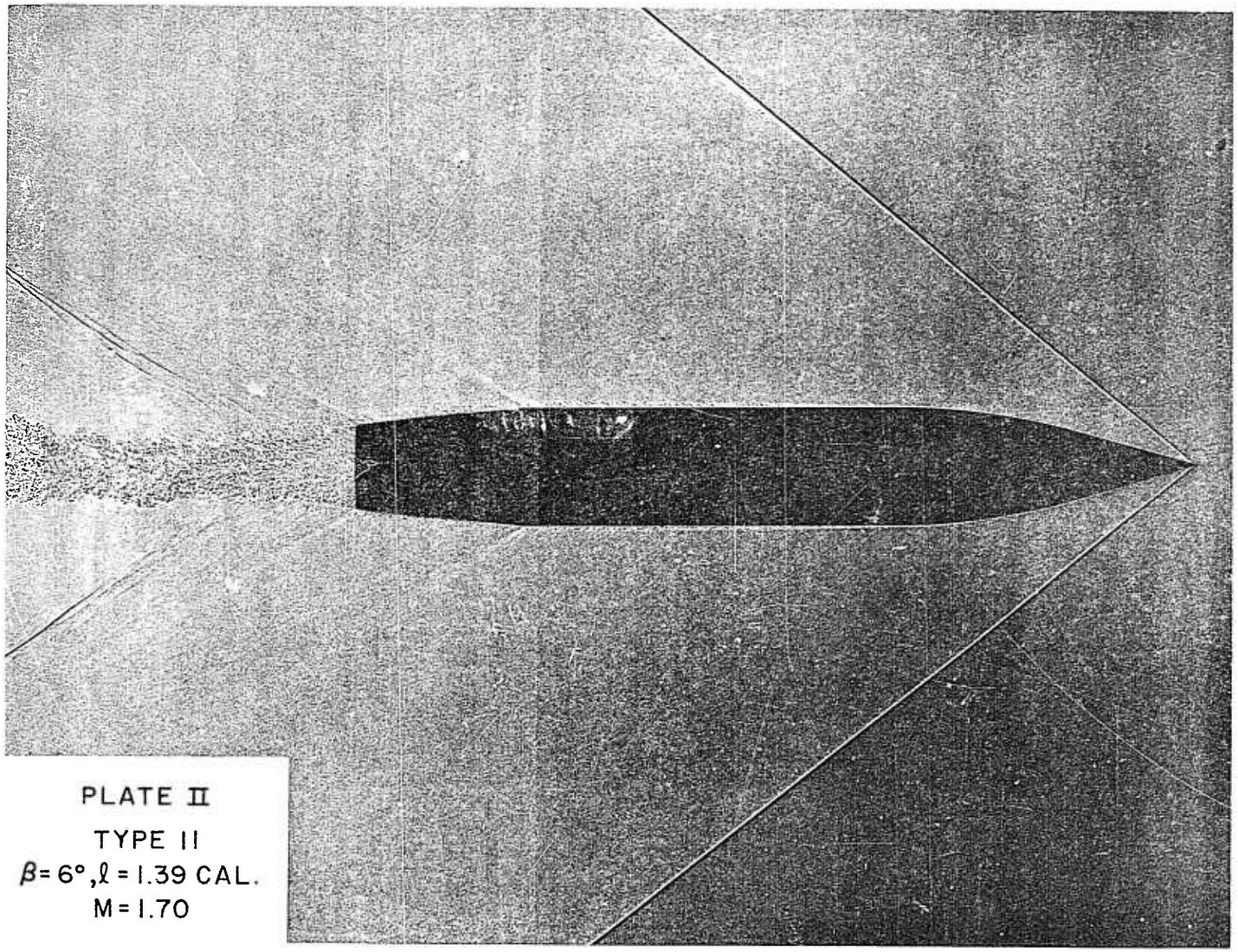

PLATE II

TYPE 11

$\beta = 6°, \ell = 1.39$ CAL.

M = 1.70

3. THE DRAG

All total drag coefficients were reduced to M = 1.70 by applying small corrections due to some scatter of actual velocities about M = 1.70, and to zero yaw. The yaw drag coefficient, as defined by the equation,

$$C_{D_o} = C_D - C_{D_{\overline{\delta^2}}} \overline{\delta^2} \qquad (1)$$

showed some slight trend with the boattail length, but no discernable difference whether the boattail was conical or ogival. The observed dependence of $C_{D_{\overline{\delta^2}}}$ on boattail length is given below:

B. T. Length, Calibers	$C_{D_{\overline{\delta^2}}}$ per radian ^{2}
0	6.6
0.5	6.4
1.0	6.1
2.0	5.1
3.0	4.3

The total drag coefficients are plotted vs. boattail length in Figure 2. It is interesting to note that the drags of models with very short boattails and large boattail angles are higher than that of the square based projectiles. This is due to a marked reduction in pressure over the short boattail. As boattail length increases the total drag rapidly diminishes but beyond a boattail length of about 1.5 calibers further decrease in drag is very slow. For boattail lengths shorter than 1.5 calibers, the ogival and concave boattails have higher drags than conical ones, the latter markedly so. As boattail length increases beyond 1.5 calibers, the ogival boattail shape approaches the conical and the two drags become similar.

At M = 1.70, for a constant conical boattail length ℓ = 0.69 caliber, as the angle is varied, minimum drag appears to be somewhere between 6 to 8 degrees, Figure 2.

TOTAL DRAG COEFFICIENT

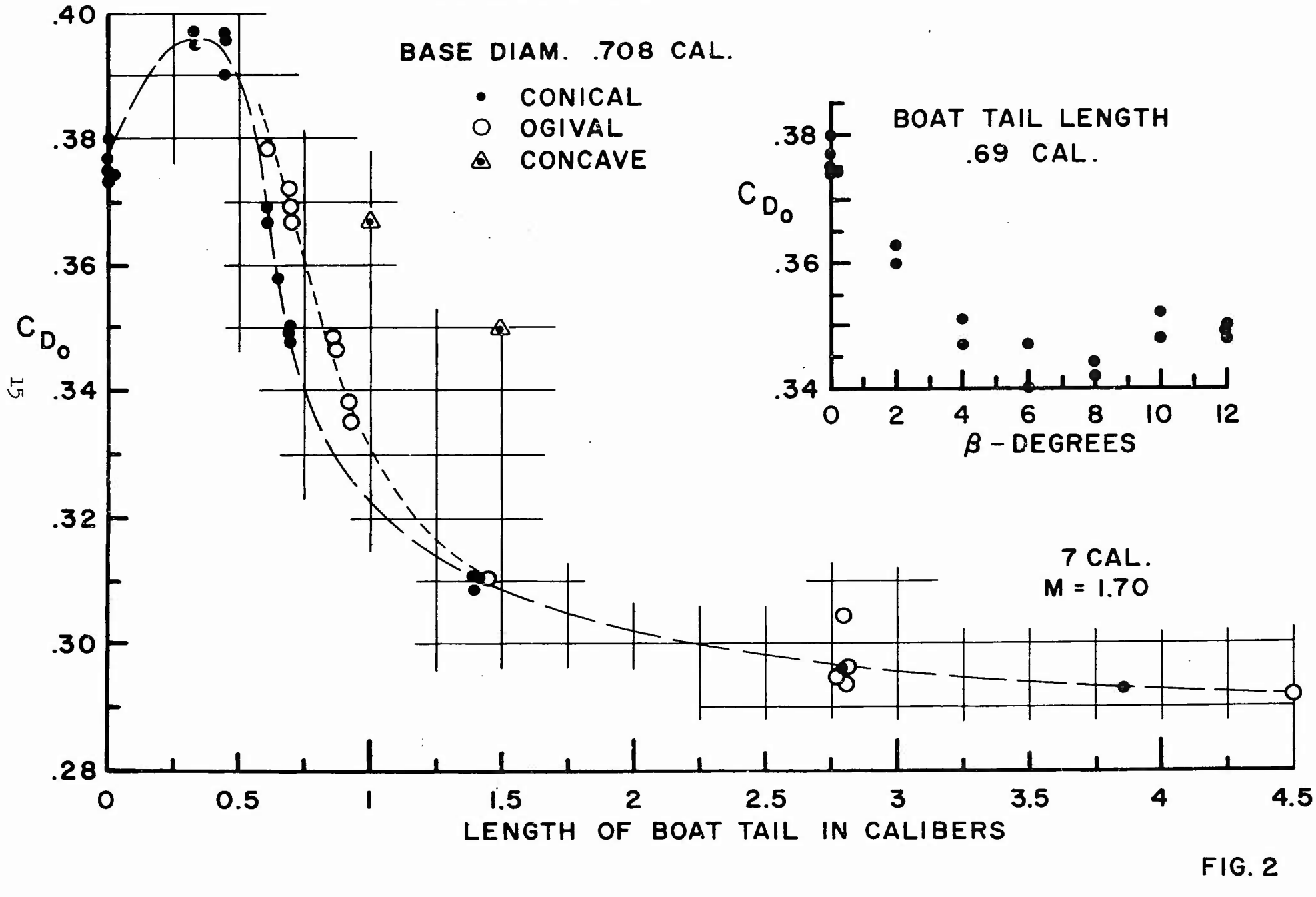

FIG. 2

3.1 Base Pressure

The total drag can be considered as composed of several component drags: head drag, boattail drag, skin friction drag, and base drag. In principle, if the first three drags are known the base drag may be obtained by subtraction, i.e.,

$$C_{DB} = C_{D_o} - C_{DH} - C_{DBT} - C_{DSF} \quad . \tag{2}$$

The base drag coefficient can be expressed as the ratio of base pressure to free-stream static pressure

$$\frac{p_b}{p_1} = 1 - \frac{\gamma M_1^2}{2} \left(\frac{D}{d_B}\right)^2 C_{DB} \tag{3}$$

where d_B is the base diameter, D is the model diameter, $M_1 = 1.70$ and $\gamma = 1.40$, or in a form of base pressure coefficient,

$$P_b = - \left(\frac{D}{d_B}\right)^2 C_{DB} \quad . \tag{4}$$

This technique has been used successfully before[4]. The base pressures so obtained were in good agreement with directly measured values in wind tunnels[5].

3.2 Head and Boattail Drags

The head and boattail drags were computed by integrating the axial component of pressures. These were obtained from theoretical pressure distributions over the models computed by the method of characteristics. The graphs of pressure distributions and of Mach number are shown in Figures 3-5. Theoretical head drag, so computed, is probably quite reliable. The boattail drag is much less certain. There are some indications that actual pressure distributions over the boattails may differ significantly from the theoretical ones.

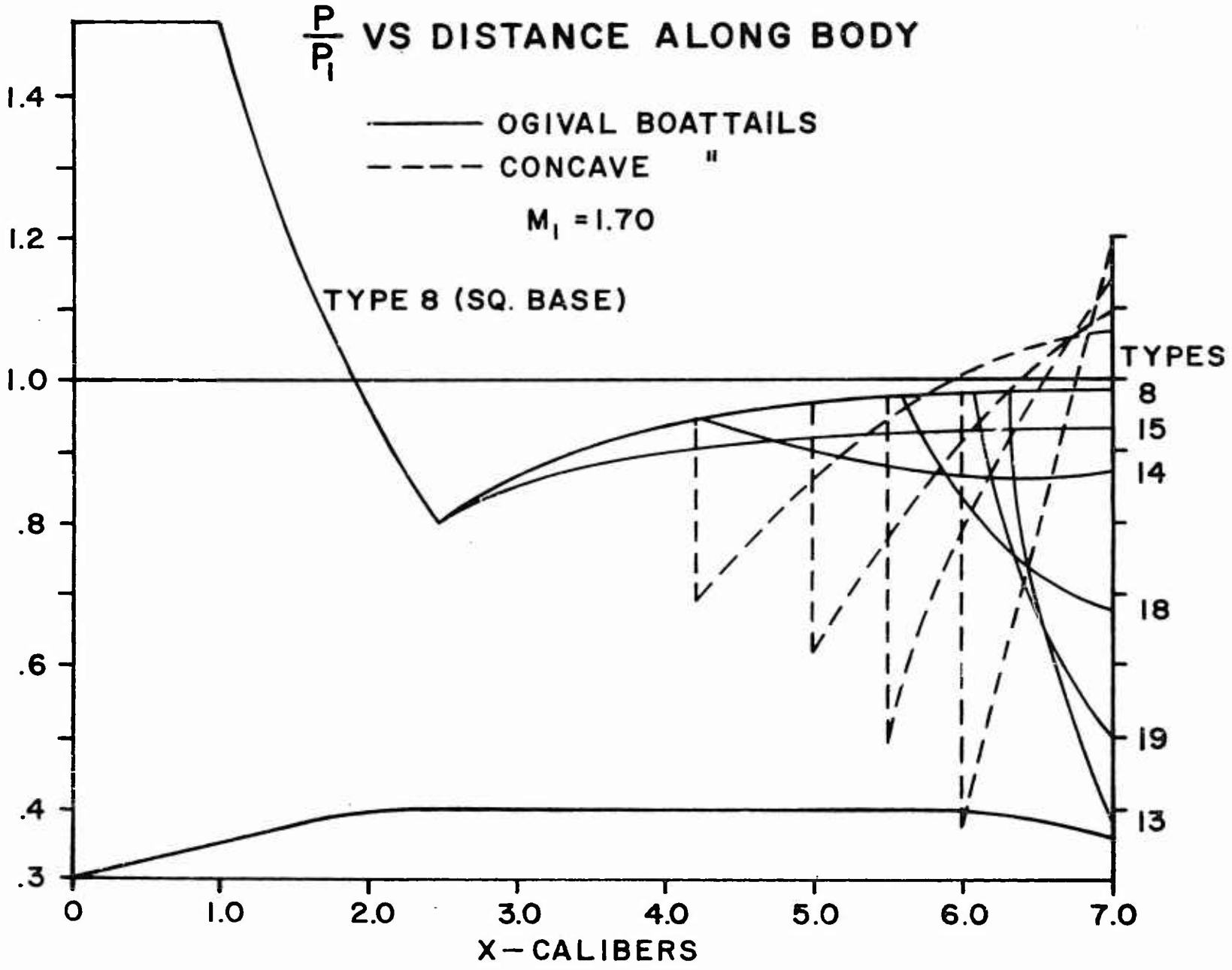
P/P1 VS DISTANCE ALONG BODY
OGIVAL BOATTAILS
CONCAVE "
M1 = 1.70
TYPE 8 (SQ. BASE)
TYPES
8
15
14
18
19
13
P/P1
1.4
1.2
1.0
.8
.6
.4
.3
0
1.0
2.0
3.0
4.0
5.0
6.0
7.0
X-CALIBERS

FIG. 3a

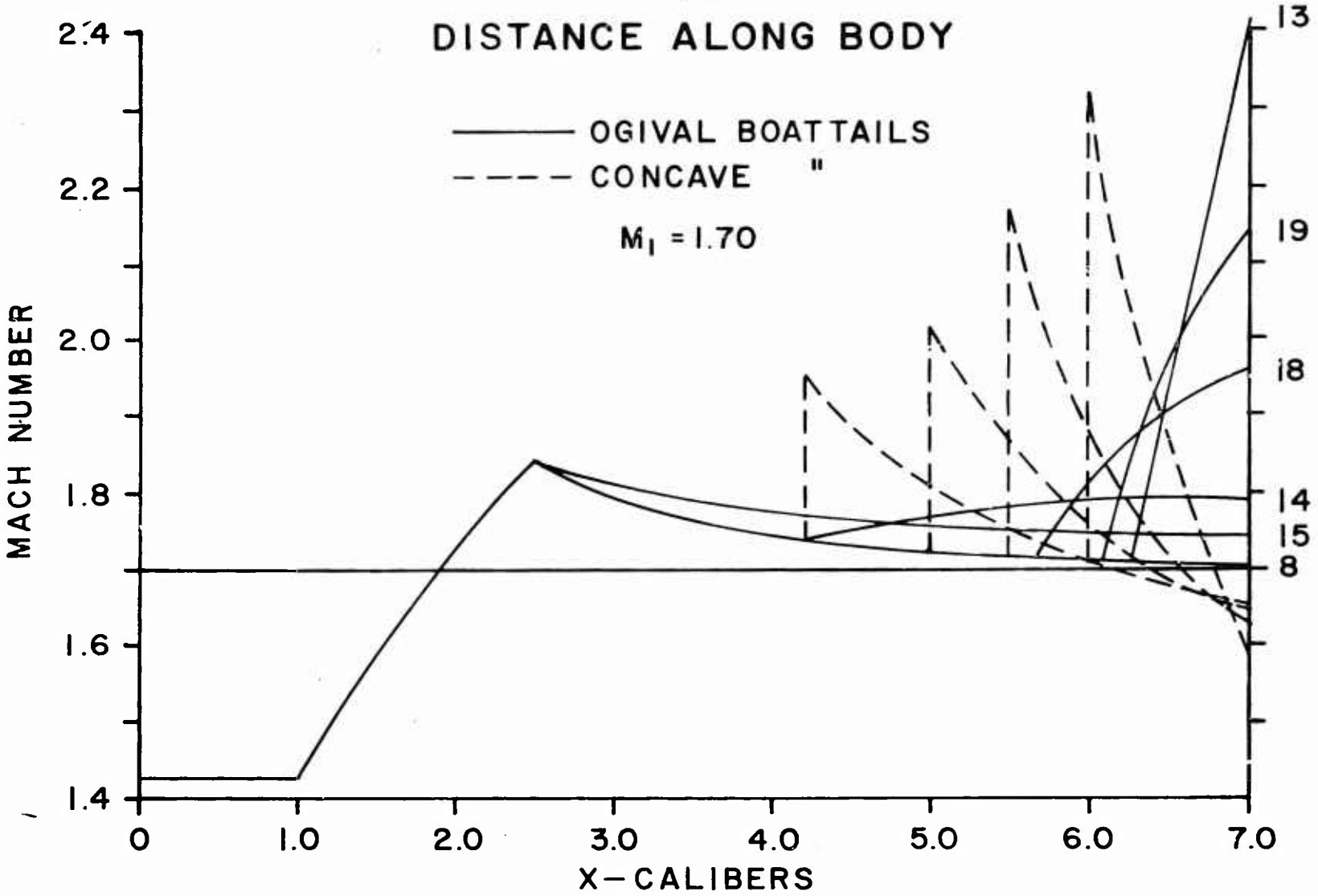
MACH NUMBER
VS
DISTANCE ALONG BODY
——— OGIVAL BOATTAILS
– – – – CONCAVE "
M_1 = 1.70
MACH NUMBER
2.4
2.2
2.0
1.8
1.6
1.4
0
1.0
2.0
3.0
4.0
5.0
6.0
7.0
X–CALIBERS
13
19
18
14
15
8

FIG. 3b

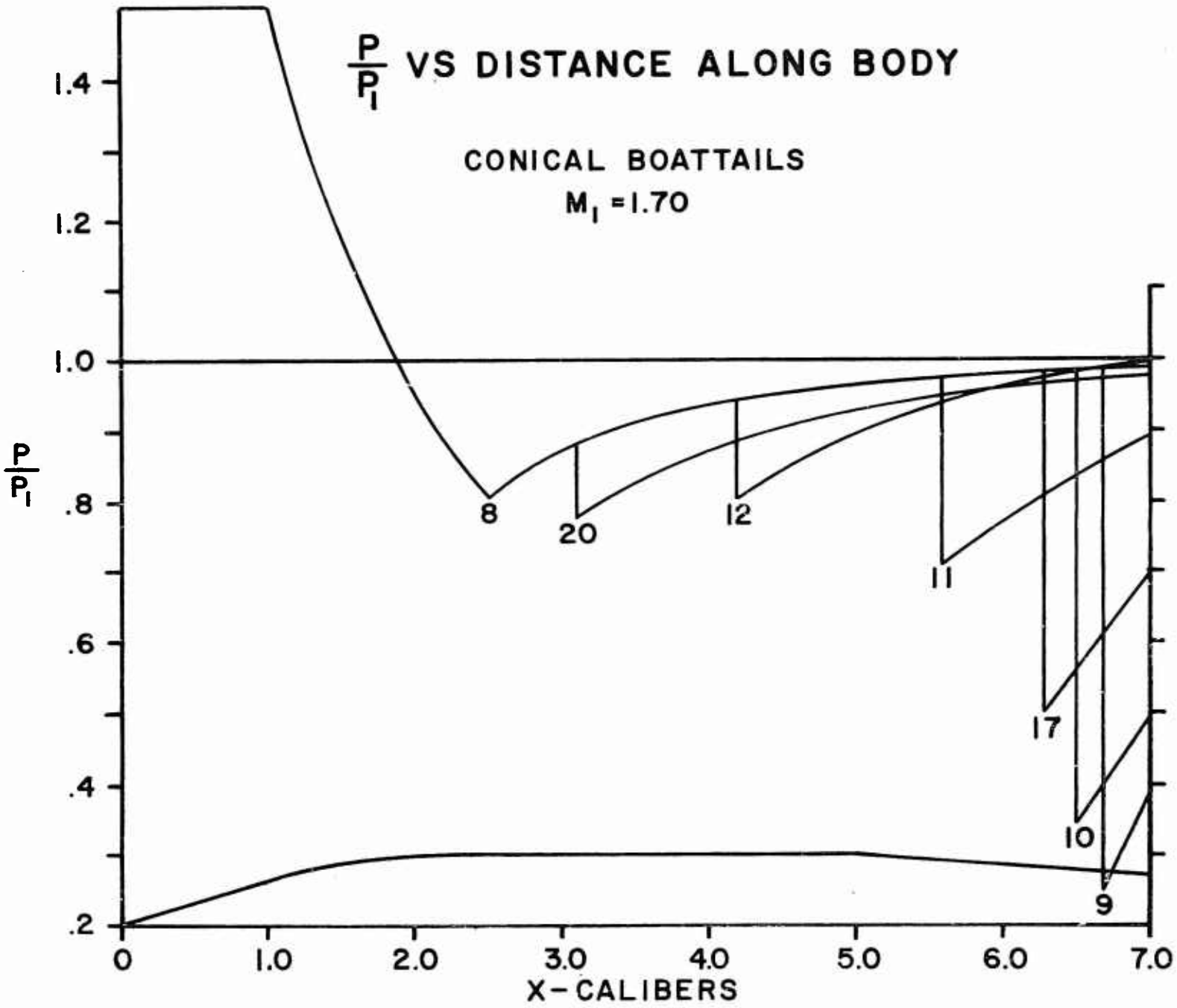
P/P1 VS DISTANCE ALONG BODY
CONICAL BOATTAILS
M1 = 1.70
P/P1
1.4
1.2
1.0
.8
.6
.4
.2
0
1.0
2.0
3.0
4.0
5.0
6.0
7.0
X-CALIBERS
8
20
12
11
17
10
9

FIG. 4a

MACH NUMBER
VS
DISTANCE ALONG BODY

CONICAL BOATTAILS

$M_1 = 1.70$

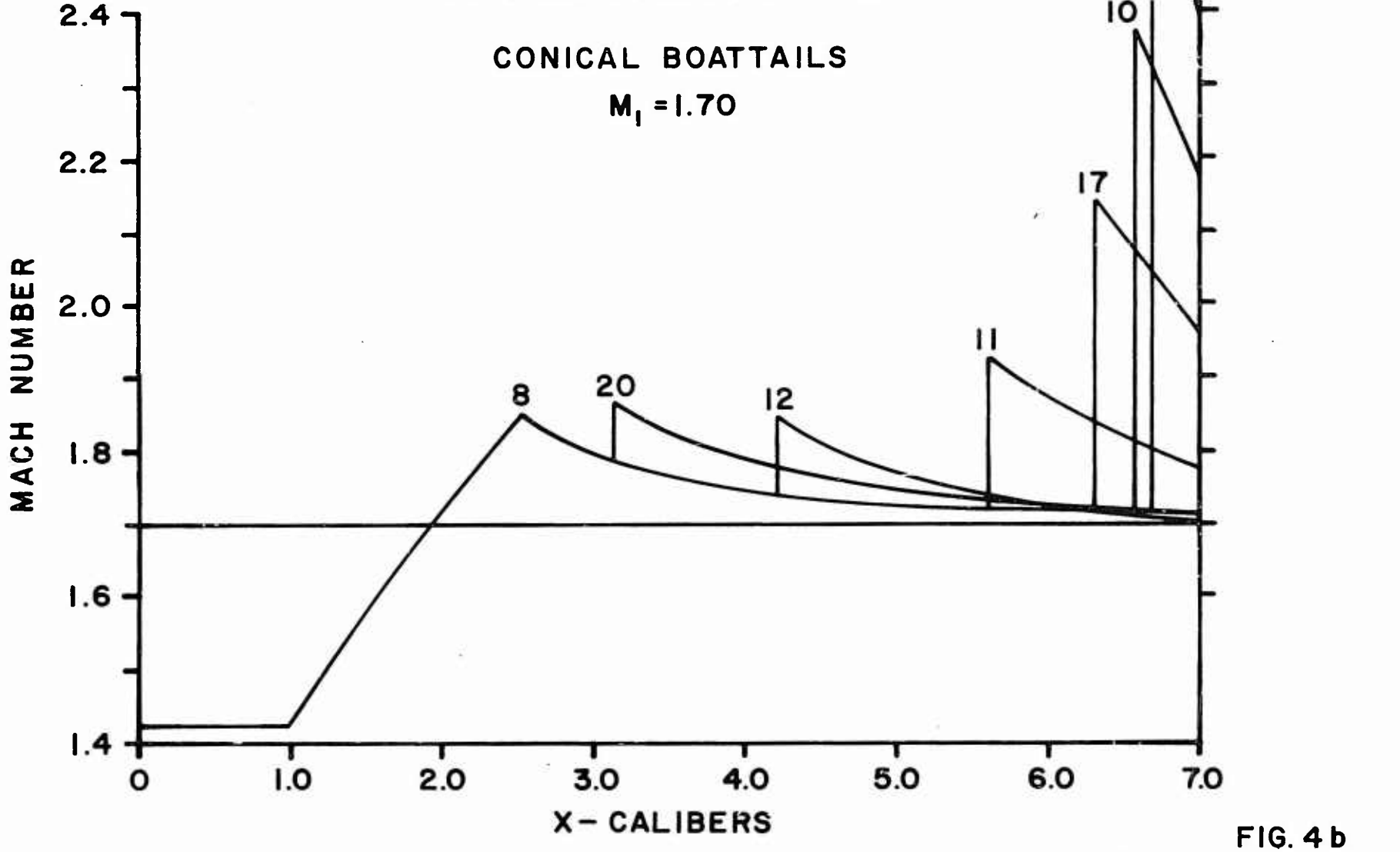

FIG. 4 b

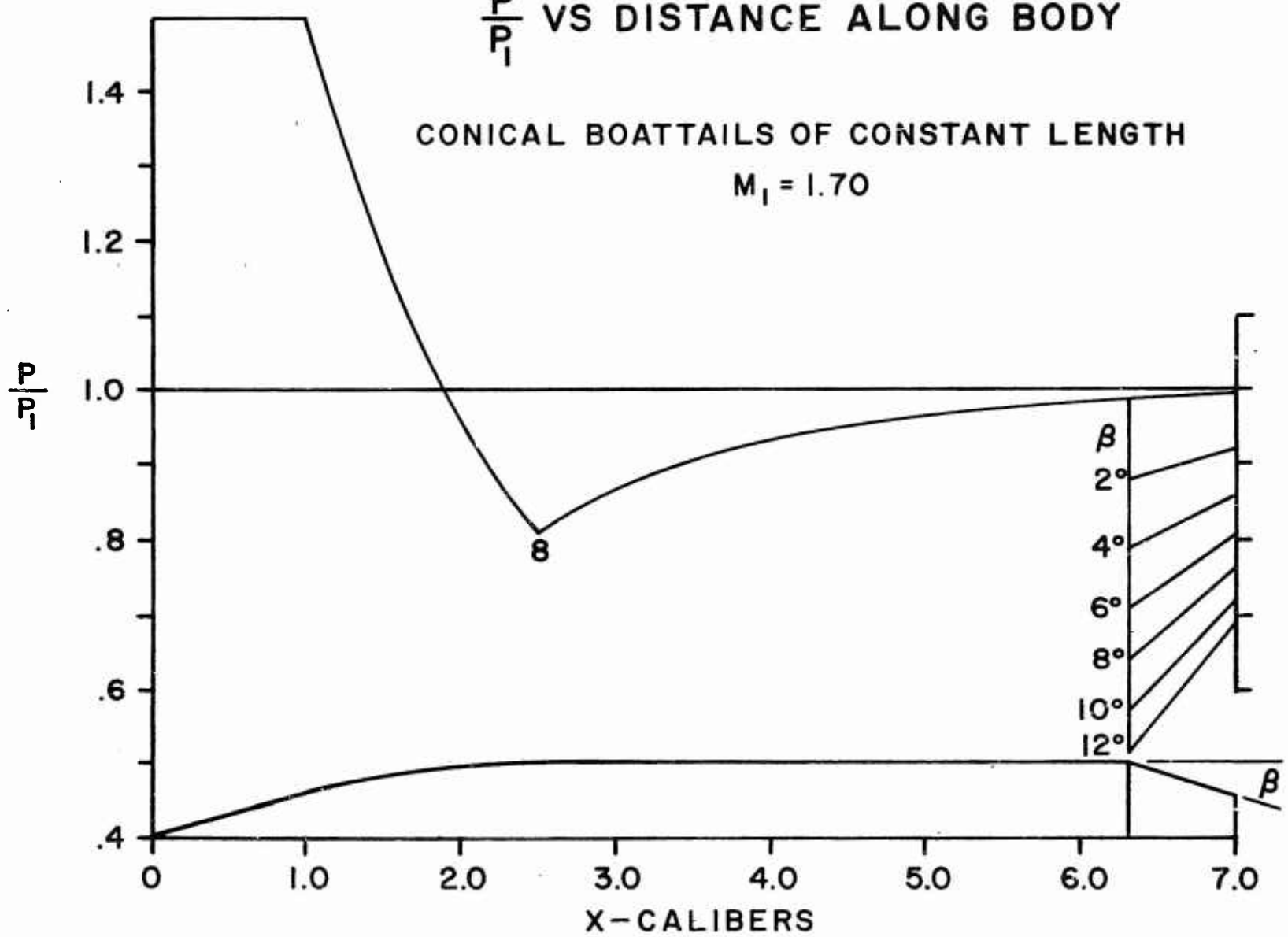
P/P1 VS DISTANCE ALONG BODY
CONICAL BOATTAILS OF CONSTANT LENGTH
M1 = 1.70
P/P1
1.4
1.2
1.0
.8
.6
.4
8
β
2°
4°
6°
8°
10°
12°
β
0
1.0
2.0
3.0
4.0
5.0
6.0
7.0
X-CALIBERS

FIG. 5a

MACH NUMBER
VS
DISTANCE ALONG BODY

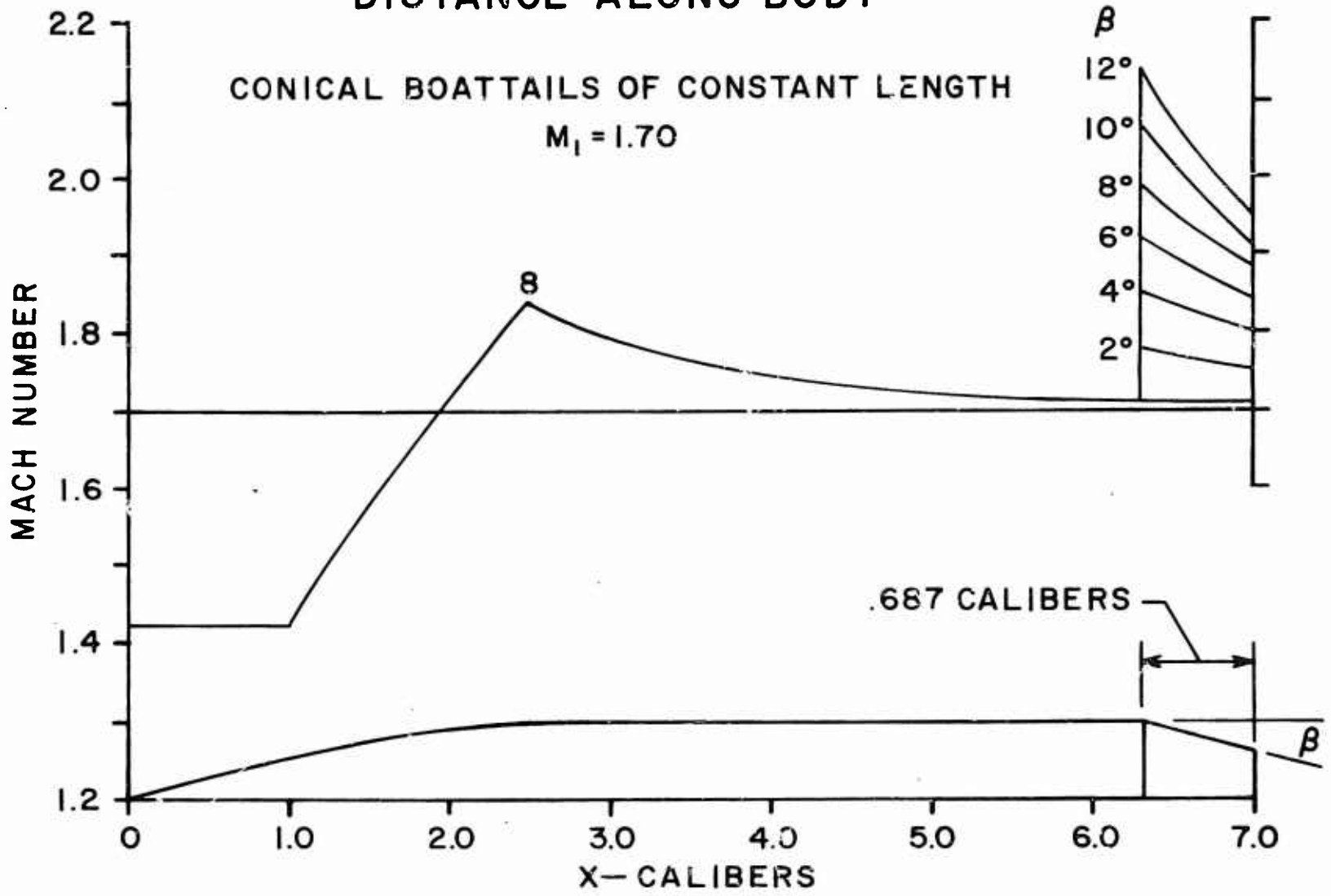

FIG. 5b

3.3 Skin Friction Drag

This drag component contributes another uncertainty to the evaluation of base drag by subtraction. Somewhat surprisingly, an application of the incompressible subsonic flat-plate formula for skin friction coefficient:

$$C_F = \frac{0.455}{(\log_{10}\mathrm{Re})\ 2.58} - \frac{1700}{\mathrm{Re}}$$

to supersonic cone-cylinder projectiles led to evaluations of base drags, by the method of subtraction, which were in good agreement with directly measured values in the wind tunnel[4]. Since in this report, we are interested primarily in the relative values of the base drags as a function of base geometry, an application of the above formula should give adequately reliable results*. All drag components are shown in Table I. If, at a later date, it becomes desirable to change the skin friction coefficient to a more appropriate value, the new base drags could be readily obtained.

The base pressures are plotted in Figure 6. The dashed lines are suggested trends. The correlation appear to be somewhat more consistent with boattail angle than with boattail length. The conical and ogival boattails with the same boattail angle at the base have essentially the same base pressure. Concave boattails have significantly lower base pressure if plotted vs. breakaway angle.

---

* *It is well known, of course, that compressibility reduces skin friction. For a turbulent boundary layer at M = 1.70, the compressible turbulent skin friction coefficient is 0.78 times its incompressible value as given by the Karman-Schonherr formula [6]. For our models the transition from laminar to turbulent boundary layer occurred, on the average, 1.3 calibers from the nose. Using, therefore, the laminar skin friction coefficient for the first 1.3 calibers, ($Re_e = 1 \times 10^6$, wetted area $A_\ell = 1.59$ sq. cal.), and a turbulent for the remainder 5.7 calibers ($Re_t = 4.36 \times 10^6$, wetted area $A_t = 17.50$ sq. cal., with 0.78 as a compressibility factor), one finds an overall skin friction drag coefficient of $C_{DSF} = .062$. This is to be compared with $C_{DSF} = .073$ obtained using the incompressible formula above and as given in Table I.*

TABLE I

Component Drag Coefficients
Conical Boattails, ℓ = 0.69 cal.

Type	β^o	ℓ	C_{D_o} (1)	$C_{D_{BT}}$	C_{DSF}	C_{DB}	$\frac{\gamma M_1^2}{2}\left(\frac{D}{d_B}\right)^2$	p_b/p_1	Sternberg p_b/p_1	M_b (2)
8	0	0	.378	0	.073	.161	2.023	.67	.64	1.71
21	2	.69	.362	.005	.073	.140	2.233	.69	.68	1.75
22	4	.69	.349	.016	.073	.116	2.476	.71	.71	1.79
23	6	.69	.344	.032	.072	.096	2.760	.74	.74	1.84
24	8	.69	.342	.051	.072	.075	3.098	.77	.78	1.87
25	10	.69	.350	.076	.072	.058	3.524	.80	.82	1.91
17	12	.69	.349	.102	.072	.031	4.035	.87	.88	1.95
				Base Diameter d_B = 0.708 Cal.						
				Conical						
9	24	.33	.396	.171	.073	.008	4.035	.97	.95	2.36
10	18	.45	.394	.146	.073	.031	4.035	.87	.88	2.17
17	12	.69	.349	.102	.072	.031	4.035	.87	.88	1.95
11	6	1.39	.310	.049	.071	.046	4.035	.81	.83	1.78
12	3	2.79	.296	.025	.068	.059	4.035	.76	.76	1.72
20	2.2	3.86	.293	.023	.066	.060	4.035	.76	.72	1.72

TABLE I (Contd)

Type	β^o	ℓ	C_{D_o} (1)	C_{DBT}	C_{DSF}	C_{DB}	$\frac{\gamma M_1^2}{2}\left(\frac{D}{d_B}\right)^2$	p_b/p_1	Sternberg p_b/p_1	M_b (2)
					Ogival					
13	24	.69	.372	.120	.073	.035	4.035	.86	.89	2.40
19	18	.92	.336	.094	.072	.026	4.035	.90	.94	2.13
18	12	1.39	.311	.065	.072	.030	4.035	.88	.89	1.95
14	6	2.79	.297	.031	.068	.054	4.035	.78	.80	1.79
15	3.7	4.50	.292	.021	.065	.062	4.035	.75	.76	1.75
					Concave					
16	16	1.00	.367	.090	.072	.061	4.035	.75	.80	1.59
26	11	1.50	.350	.064	.072	.070	4.035	.72	.76	1.62

(1) Head drag C_{DH} = .144 for all models.

(2) M_b = Mach number at the base.

BASE PRESSURE

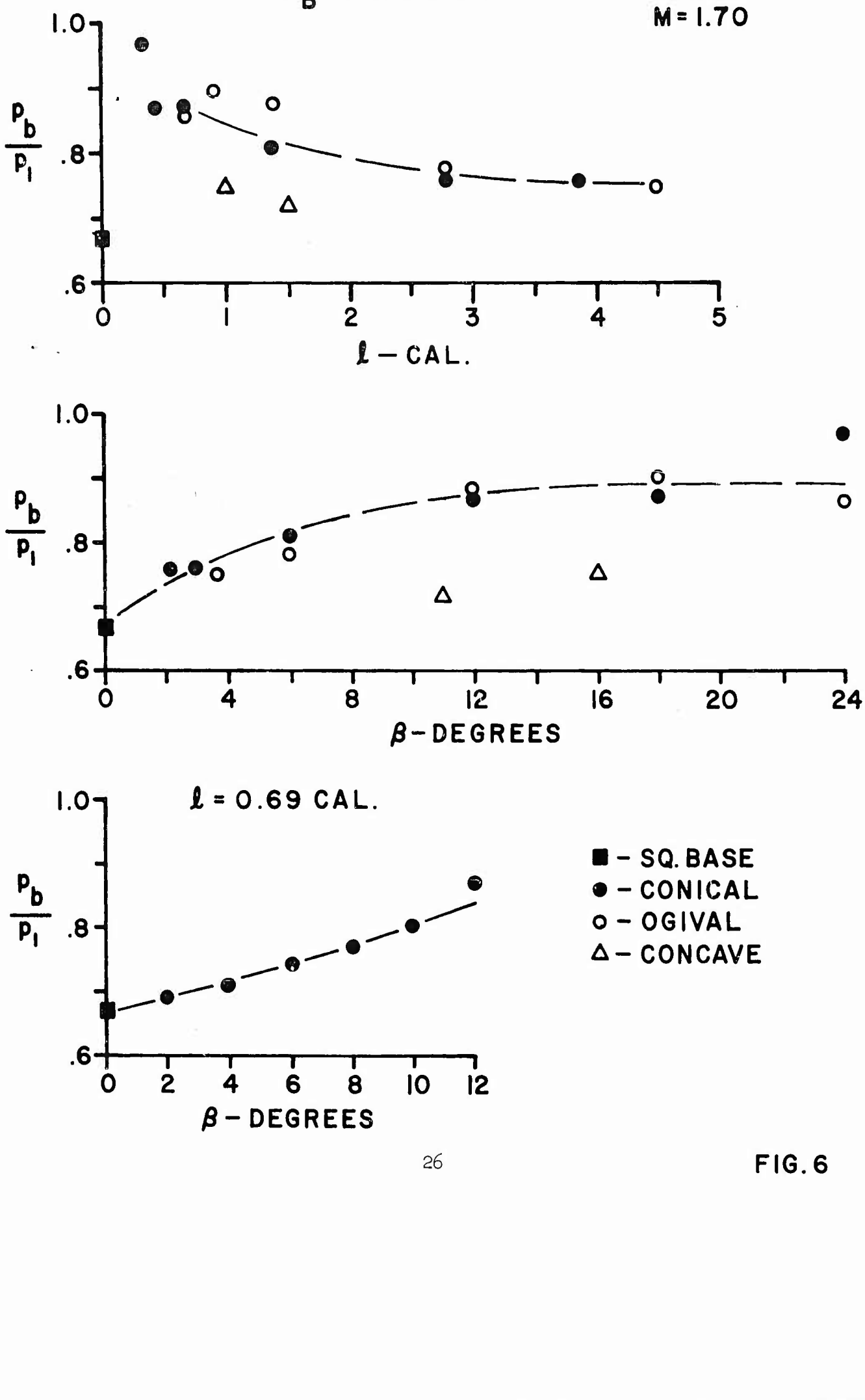

FIG. 6

3.4 Sternberg's Method of Estimating Base Pressure of Boattailed Projectiles

A full description of Sternberg's suggestion is to be found in his memorandum to Kent, which is reproduced in Appendix 1. Essentially, as far as the present problem is concerned and as a first approximation, Sternberg assumes that the base pressure will be determined by the local flow conditions at the base. The local conditions are described in terms of an "effective Mach number, M_{eff}" and a static pressure corresponding to M_{eff}. The effective Mach number is the Mach number of parallel flow which would reach the local Mach number at the base of a boattailed projectile when expanded to the surface angle two dimensionally. If one has, moreover, an experimentally determined relation between the ratio of base pressure to local static pressure at the base of square based projectile for various "effective"Mach numbers, i.e., Mach number at the base, then the base pressure for boattailed projectiles can be readily estimated. Fortunately, such a relation is available in Reference (4). There we are given a ratio of base pressure to free-stream static pressure for various free-stream Mach numbers. The projectile was a square based cone-cylinder, 5 calibers long with 19° included angle conical head. For this projectile, at Mach numbers in the vicinity of 1.7, the base Mach number and static pressure were very nearly those of the free-stream. At $M \sim 1.7$, the entropy loss thru the conical shock is negligible, hence the total pressures at the base and in the free-stream are nearly the same. Therefore, one can regard the data given in Reference (4), i.e., the observed ratio of the base pressure to the free-stream static pressure vs M, as a relation between the base pressure and the local static pressure vs local Mach number at the base, or M_{eff}. The observed relation can be well fitted by the following expression

$$\frac{p_b}{p'} = 1.108 - 0.309\, M_{eff} + 0.0241\, M_{eff}^2$$

where p' is the static pressure at the base.

To illustrate the application of the method, we shall apply it to the projectile type 25 which has a conical boattail length of 0.69 calibers and a boattail angle of 10°. From Figure 5b we find that the Mach number at the end of this boattail is 1.92.

Using, for example, NACA's "Equations, Tables and Charts for Compressible Flow," Report 1135 (1953) we find:

a. Prandtl-Meyer angle corresponding to M = 1.92 is 24.151°.

b. For the 10° boattail angle, the effective Mach number ($\nu = 24.151^{\circ} - 10^{\circ} = 14.151^{\circ}$) is $M_{eff} = 1.58$ with corresponding static to total pressure ratio

$$\frac{p'}{p_t} = .2437$$

c. The ratio of free stream static to total pressure at M = 1.70 is

$$\frac{p_1}{p_t} = .2026$$

d. The "observed" ratio of base pressure to local static pressure at M_{eff}, Equation (10),

$$\frac{p_b}{p'} = .68$$

e. Thus we have

$$\frac{p_b}{p_1} = \left(\frac{p_b}{p'}\right)\left(\frac{p'}{p_t}\right)\left(\frac{p_t}{p_1}\right)$$

$$= (.68)\left(\frac{.2437}{.2026}\right) = .82 \ .$$

By subtraction of drag components from the total drag, the same ratio, see Table I, is 0.80. The base pressures for all models, as estimated by Sternberg's method, outlined above, are given in Table I. The agreement between the subtraction and Sternberg methods, at this Mach

number, is very good. The average disagreement, as measured by the standard deviation is less than 3 percent. However, this agreement might be fortuitous. If one were to use a compressible skin friction coefficient in the analysis of range data, than the agreement with Sternberg's, as expressed by the standard deviation, would be 7 percent. On the whole, therefore, neither the method of subtraction nor Sternberg's method should be considered as to give an estimate of base pressure to better than, say, 10 percent.

3.5 Wind Tunnel Measurements

Two models with boattail length of 1.39 calibers, one conical, Type 11, and another ogival (convex), Type 18, were recently tested in the wind tunnel at Mach numbers of 2.00 and 1.73. Extrapolated to M = 1.70, the Reynolds number, based on overall length, was adjusted to be the same as in free flight, i.e., 5.36×10^6. It was found necessary, however, to induce an artificial transition of the boundary layer by a narrow band of fine sand so as to simulate the position of the transition in free-flight. At M = 1.70, and reduced to zero roughness, the results are as follows:

	C_{D_o}		p_b/p_1	
B. T.	Conical	Ogival	Conical	Ogival
W. T.	.307	.322	.86	.88
Range	.310	.311	.81	.88

The agreement is reasonably good, i.e., within 5 percent or so.

4. OTHER AERODYNAMIC CHARACTERISTICS

4.1 C_{L_α}

Lift coefficients were determined from the swerving motion of the center of mass. It is well known in range work that this method is not as accurate as the two center of mass positions, for example. Nevertheless, they show a generally decreasing trend both with the increasing length of the boattail and boattail angle, Figures 7a and b.

LIFT AND DAMPING MOMENT COEFFICIENTS

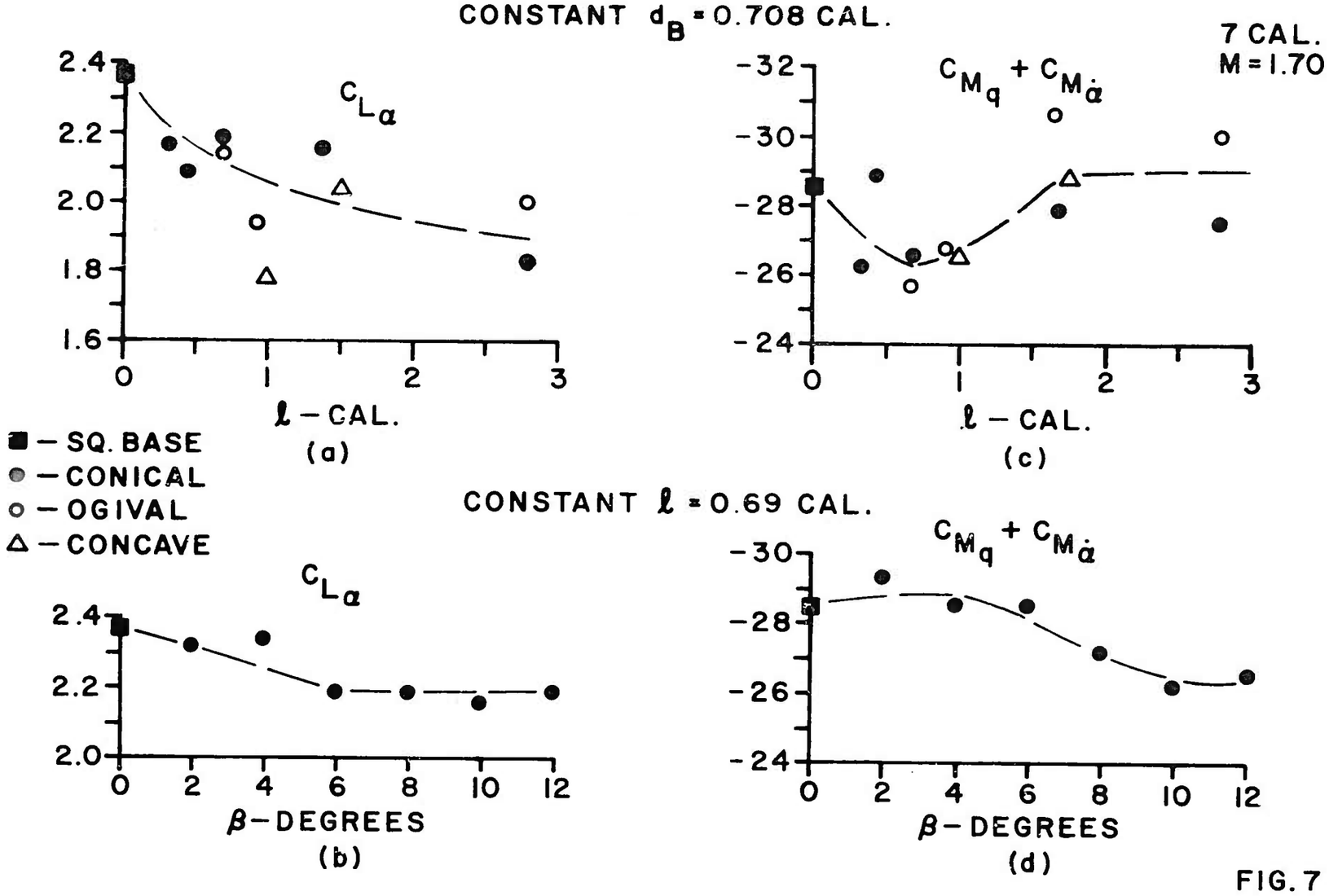

FIG. 7

4.2 $C_{Mq} + C_{M_{\dot{\alpha}}}$

The yaw damping moments show an increasing trend at shorter boattail lengths, but seem to recover at lengths in excess of 1.5 calibers. Whether, at these lengths, the observed difference between ogival and conical boattails is real or due to scatter is difficult to say. For constant boattail length models, up to boattail angles of 6°, the yaw damping moment appears to remain the same as for the square base and then increases. Figures 7c and d.

4.3 $C_{M_{p\alpha}}$

The most significant change with boattail length and angle occurs in Magnus torque coefficient, Figures 8a and c. This is especially startling for very short boattails, $\ell = 0.33$ to $\ell = 0.45$ calibers. Such large changes in the Magnus torque coefficient have a profound effect on the yaw damping properties of the models.

Some of this change may be due to a slight forward shift of the center of mass position as boattail lengthens. The change in the center of mass position, $\frac{d(c.m.)}{d\ell}$, is about 0.1 per one caliber of boattail length for conical boattails and is slightly less for ogival boattails. The Magnus force coefficient, $C_{N_{p\alpha}}$, is about 0.6. Thus the Magnus torque coefficient may be expected to increase by about .06 per caliber of boattail. The observed changes are considerably in excess of this rate suggesting a real effect of the boattail.

The influence of the boattail on Magnus torque coefficient is shown even more clearly for models with constant boattail length, 0.69 caliber, but variable angle, Figure 8b. In this case, the center of mass position changes only at a rate of .006 calibers per degree of boattail angle with an expected rate of increase in the Magnus torque of about .004 per degree of boattail angle. The observed rate is about ten times as great.

MAGNUS TORQUE COEFFICIENT

CONSTANT $d_B = 0.708$ CAL.

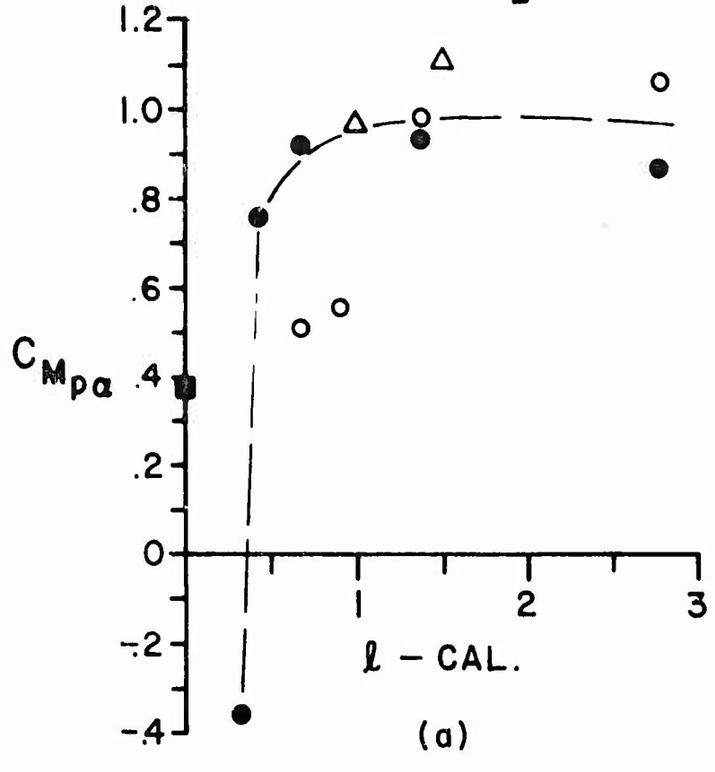

7 CAL.
M = 1.70

■ – SQ. BASE
● – CONICAL
○ – OGIVAL
△ – CONCAVE

(a)

CONSTANT $\ell = 0.69$ CAL.

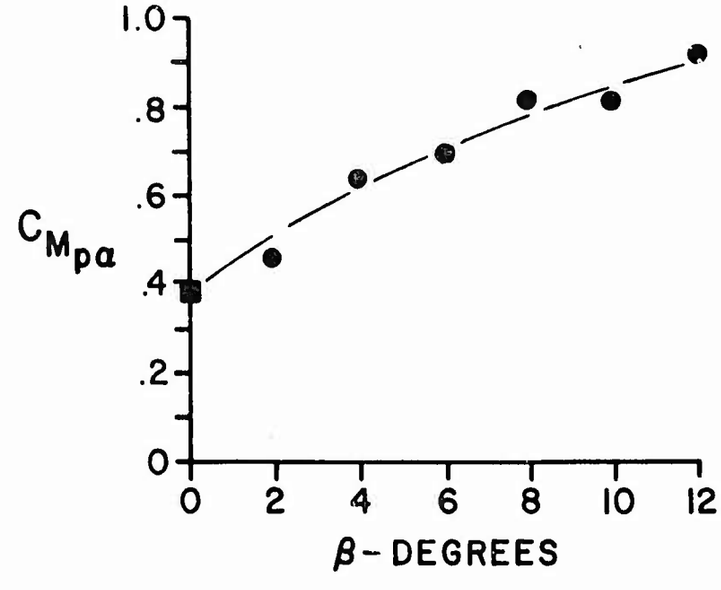

(b)

FIG. 8

MAGNUS TORQUE COEFFICIENT

CONSTANT $d_B = 0.708$ CAL.

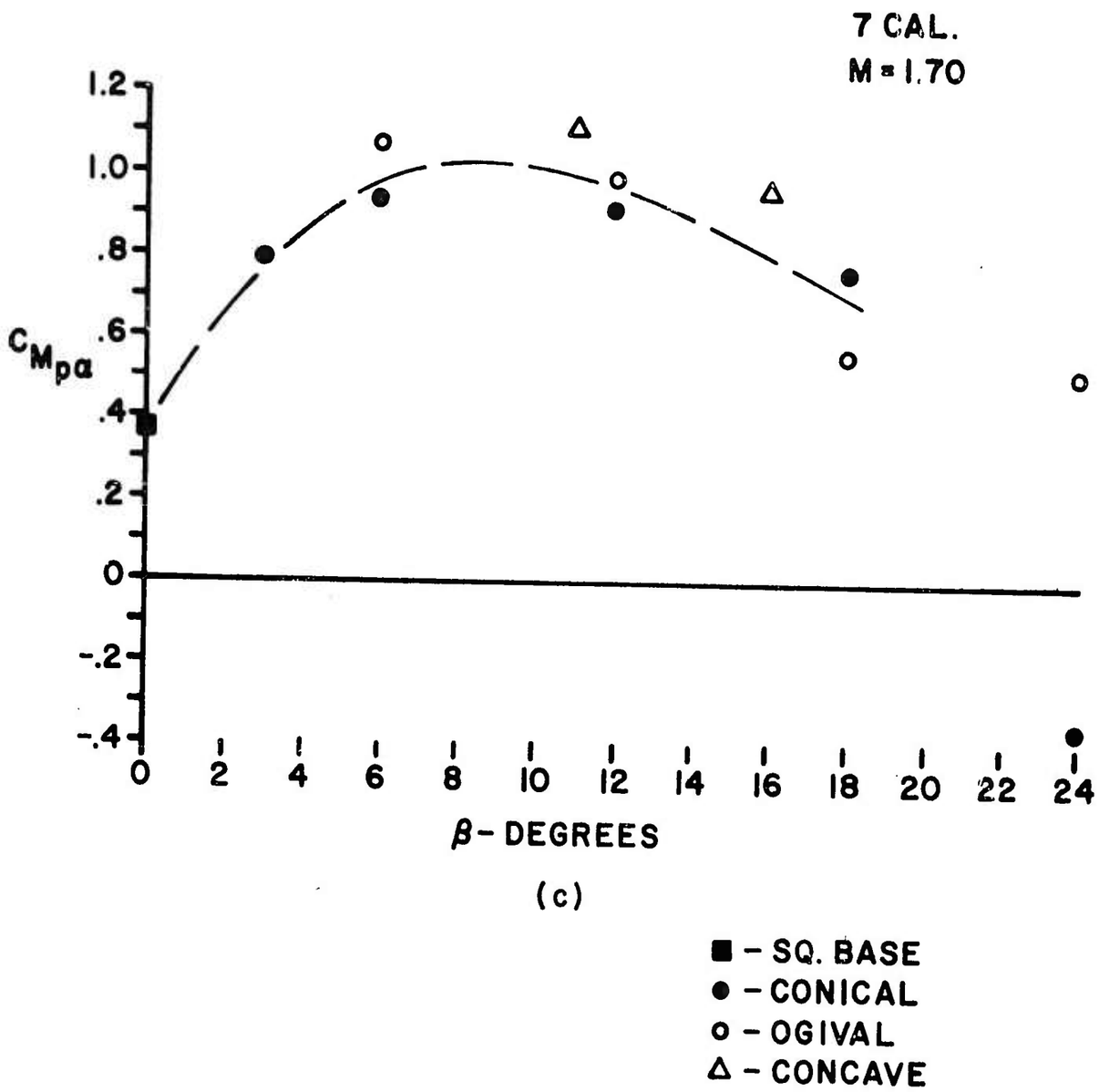

(c)

■ - SQ. BASE
● - CONICAL
o - OGIVAL
△ - CONCAVE

FIG. 8

4.4 The Center of Pressure

The center of pressure of the normal force is moving forward with increasing boattail length and boattail angle, Figure 9.

4.5 Yaw Damping Rates

For a rigid shell the yaw damping rates, per caliber of travel, are given by the following expression[3]:

$$\alpha_{1,2} = 1/2\left[\left(1 \pm \frac{1}{\sigma}\right) H \mp \frac{2}{\sigma} T + \frac{(1 \pm \sigma)}{\sigma^2} D\right]$$

where

$$H = \frac{\rho S d}{2m}\left[C_{L_\alpha} - C_D - k_t^{-2}\left(C_{M_q} + C_{M_{\dot{\alpha}}}\right)\right]$$

$$T = \frac{\rho S d}{2m}\left[C_{L_\alpha} + k_a^{-2} C_{M_{p\alpha}}\right]$$

$$D = \frac{\rho S d}{2m}\left[C_D + k_a^{-2} C_{\ell_p}\right]$$

$$\sigma = \sqrt{1 - \frac{1}{s}} \qquad s = \frac{\bar{\nu}^2}{4M} \quad \text{gyroscopic stability factor}$$

$$M = \frac{\rho S d}{2m} k_t^{-2} C_{M_\alpha} \qquad k_a^{-2} = \frac{md^2}{I_x} \qquad k_t^{-2} = \frac{md^2}{I_y}$$

$$\bar{\nu} = \frac{I_x}{I_y}\nu \qquad \bar{\nu} = \frac{I_x}{I_y}\frac{2\pi}{n} = \frac{I_x}{I_y}\frac{pd}{u}$$

and ρ = air density

S = cross-sectional area = $\frac{\pi d^2}{4}$

n = twist of rifling in calibers per turn

p, u = axial spin and velocity respectively

m = mass

I_x, I_y = polar and transverse moments of inertia.

CENTER OF PRESSURE

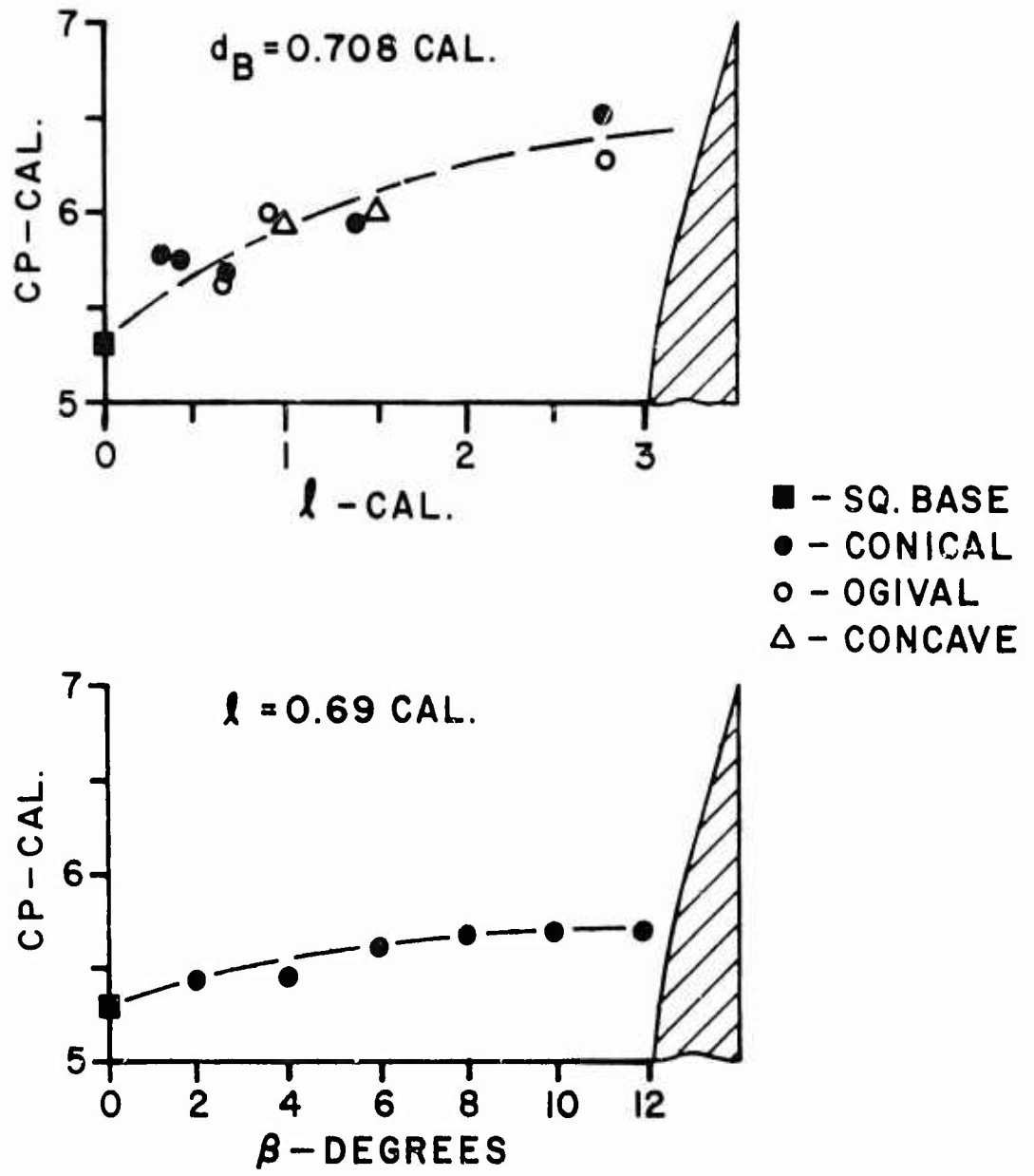

FIG. 9

In range firings, the yaw damping rates are determined as logarithmic decrements of measured amplitudes of oscillatory motion of each component of yaw. For dynamic stability the condition

$$\alpha_{1,2} > 0$$

must be staisfied.

Plots of α_1 and α_2 for models with various boattails and angles are shown in Figures 10 a and b. The results are somewhat startling. The behavior of the damping rates definitely reflects the behavior of the Magnus torque coefficient. The nutational component is progressively becoming less stable because of the increasing value of the T term due to an increase in the Magnus torque. The dominating influence of this term is clearly shown in Figure 10 b where the trend of the damping rates is very similar to the trend of the Magnus torque coefficient, Figure 8 b.

4.6 A Comparison of 7 Calibers AN Rocket Model with Present Square Base Model

Finally, it is of interest to compare the relative importance of varying head shape and boattailing on aerodynamic characteristics.

In Reference (7), aerodynamic characteristics of 5 , 7 , and 9 caliber long models of the "Army - Navy spinner rocket" are given for various Mach numbers. The models consisted of a 2-caliber long head, defined by a secant ogive of minimum drag, and a cylindrical body. The present model has a 2.5-caliber head and 4.5-caliber body.

A comparison of the aerodynamic characteristics of the two models is shown on the next page.

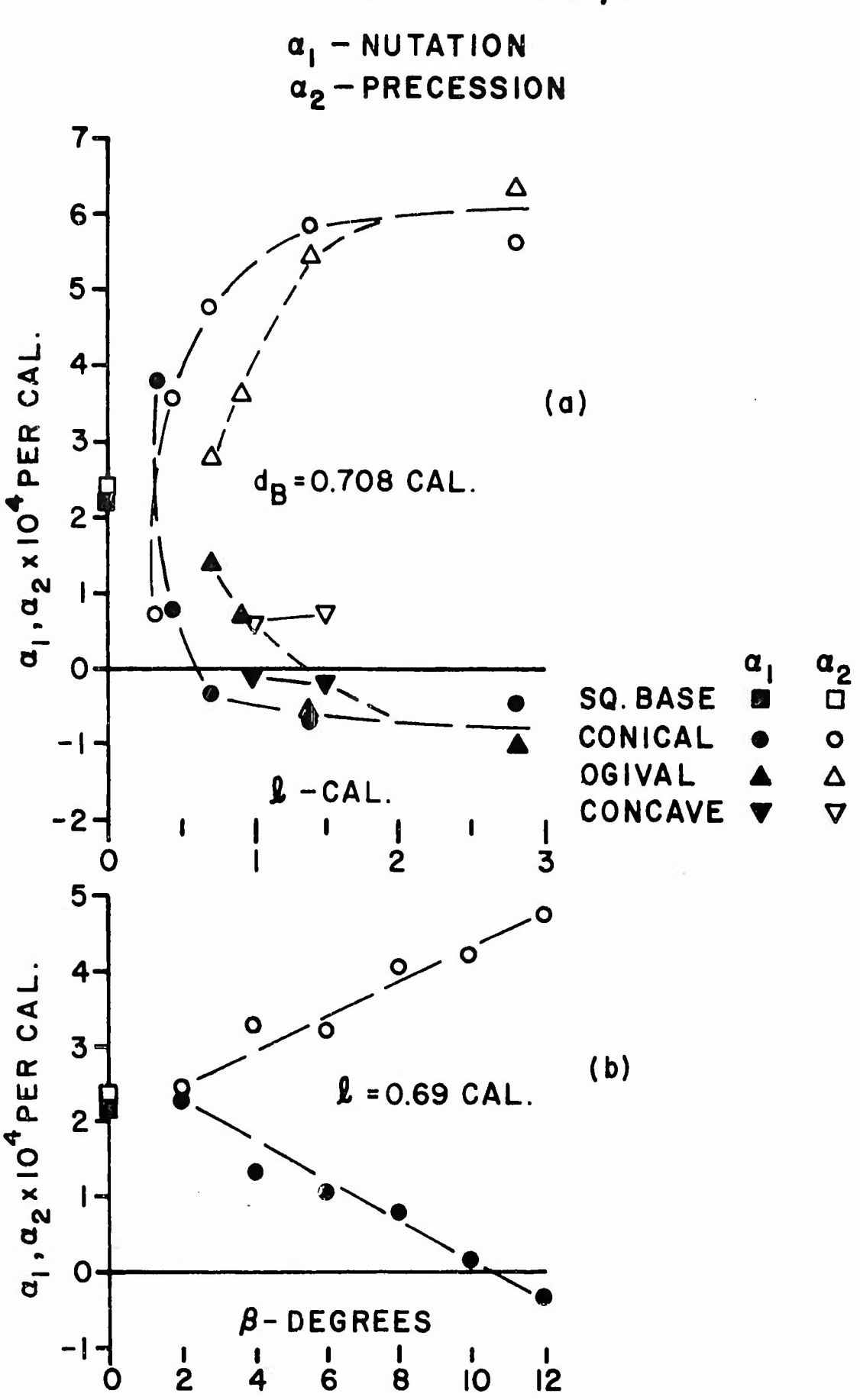
YAW DAMPING RATES, $e^{-\alpha_i p}$
α_1 – NUTATION
α_2 – PRECESSION
$\alpha_1, \alpha_2 \times 10^4$ PER CAL.
d_B = 0.708 CAL.
(a)
ℓ – CAL.
α_1 α_2
SQ. BASE
CONICAL
OGIVAL
CONCAVE
ℓ = 0.69 CAL.
(b)
β – DEGREES

FIG. 10

Square base, 7 cal. models, M = 1.70*

	AN Rocket	Present Model, Type 8
C_{D_o}	.395	.378
p_b/p_1	.64	.67
$C_{L\alpha}$	2.43	2.37
CP cal. from nose	1.61	1.67
$C_{Mq} + C_{M\dot{\alpha}}$	-29	-28.5
$C_{M_{p\alpha}}$	.5	.38
c.m., cal. from base	2.90	2.90

The higher drag coefficient for the AN rocket model is due to its shorter head of 2 calibers vs. 2.5 calibers of the present model. Although the head of the present model is not that of the minimum drag shape, its increased length reduced its overall drag. The general agreement is quite good, suggesting that the indicated differences in the head shapes produce relatively minor differences in their aerodynamic characteristics. Boattailing causes much more significant variations.

---

* *It was customary in earlier works at BRL to report the results of aerodynamic tests in terms of the ballistic coefficients, K_D, K_L, etc., rather than the aerodynamic coefficients, C_D, C_{L_α}, etc. For some years now, the practice is to use the aerodynamic nomenclature. Unfortunately, there is a difference between earlier and present practices in use of the conversion factors from one system into another. For certain coefficients, and these are marked by an asterisk below, the conversion factor used earlier was $16/\pi$; in present practice it is $8/\pi$. Thus, care should be exercised in comparing earlier with more recent results. The following current system is used in this report:*

$$C_D = (8/\pi)K_D \qquad C_{M_q} + C_{M_{\dot{\alpha}}} = -(8/\pi)(K_H - K_{MA})^*$$

$$C_{L_\alpha} = (8/\pi)K_L \qquad C_{M_{p\alpha}} = -(8/\pi)K_T^*$$

$$C_{M_\alpha} = (8/\pi)K_M \qquad C_{\ell_p} = -(8/\pi)K_A^*$$

5. CONCLUDING REMARKS

a. Conical boattails still appear to be superior to either ogival (convex) or concave shapes. Slightly higher drags of models with ogival boattails, for boattails shorter than 1.5 calibers, are largely due to higher boattail drag component.

b. The base drags, for conical and ogival boattails, appear to correlate better with the base approach angle rather than with the boattail length. But in either case, whether conical or ogival, the base drags for these two types of boattail shapes do not appear to differ very much.

c. For bodies of high fineness ratios, care should be exercised in designing boattailed configurations because of significant effects of boattailing on aerodynamic characteristics relative to square based designs. Magnus torque coefficient appears to be particularly sensitive to boattailing, so much so that an improper design of the boattail may make the configuration dynamically unstable.

ACKNOWLEDGEMENTS

The auther is grateful to Dr. J. Sternberg for permission to reproduce his memorandum to Kent and to Mr. R. H. Krieger for wind tunnel testing of the two models.

Early analysis of part of the data was done by Mr. Eliot Ranard, then a Private in the U. S. Army, assigned to the Ballistic Research Laboratories. Most of the data were reworked by Mrs. Karolyn Krial.

B. G. KARPOV

REFERENCES

1. Dickinson, E. The Effect of Boattailing on the Drag Coefficient of Cone-Cylinder Projectile at Supersonic Velocities. Ballistic Research Laboratories Memorandum Report No. 842, November, 1954.

2. Braun, W. F. The Free Flight Aerodynamics Range. Ballistic Research Laboratories Report No. 1048, July, 1958.

3. Murphy, C. H. Data Reduction for the Free Flight Spark Range. Ballistic Research Laboratories Report No. 900, February, 1954.

4. Charters, A. C. and Turetsky, R. A. Determination of Base Pressure from Free-Flight Data. Ballistic Research Laboratories Report No. 653, March, 1948.

5. Chapman, D. R. An Analysis of Base Pressure at Supersonic Velocities and Comparison with Experiment. NASA TN 2137, July, 1950.

6. Chapman, D. R. and Kester, R. H. Turbulent Boundary-Layer Skin Friction Measurements in Axial Flow Along Cylinders at Mach Numbers Between 0.5 and 3.6. NASA TN 3097, March, 1954.

7. Murphy, C. H. and Schmidt, L. E. The Effects of Length on the Aerodynamic Characteristics of Bodies of Revolution in Supersonic Flight. Ballistic Research Laboratories Report No. 876, 1953.

APPENDIX

COPY

FROM: J. Sternberg 28 May 1948

TO: R H. Kent

SUBJECT: Effect of boattail on the base pressure

Summary

A qualitative analysis of the effect of boattails with turbulent boundary layer (species-finis) has engendered an experimental wind tunnel and free flight program. Employing a simplified flow mechanism, the base pressure for a two dimensional model appear independent of the boattail angle for a sizable angular variation. As a first approximation, this result is utilized to estimate the base pressure for axially symmetric flow, while the flow features insisting on a more sophisticated approx-mation are described in detail.

1. Viscous Effects

Experimental data on bodies of revolution with turbulent boundary layers shows a relatively small variation of the base pressure with Reynold's number. For example, for a R. N. variation of 5, over the range of values obtained in the wind tunnel, the change in base pressure is of a smaller order of magnitude than the changes which might be expected due to boattailing. In order to compare the base pressure for dissimilar models, suitable boundary layer parameters, such as the dis-placement and momentum thickness referred to the model base diameter, should be chosen. For similar models, including both square bases and boattails, an increase of R. N. by a factor of 5 would change the ratio of such a defining length approximately 1.4 times. It is both reasonable and convenient to assume that in going from the squre based bodies to the boattailed bodies, this ratio would not change by more than a factor of 1.5, which, in effect, means that R. N. influences on the comparisons can be approximately neglected. However, if the base diameter is small, such a defining length would be increased both by the decrease in base size and the divergence of the boundary layer streamlines and its changes can no longer be neglected. Rough estimates of variations in base pressure from this source can be made if desirable.

2. Some Observation on Flow Stability

The wake flow has been disturbed in two different ways. First, objects of a two parameter family have been placed in the model wake. Constant diameter rods attached to the model base, if of sufficient length, decrease the base pressure, unless the diameter of the rod approaches the diameter of the model, when the base pressure must increase towards the pressure on the side of the model. The flow appears stable for changes in rod size, changing with reasonable uniformity. Yet, if large objects, of the size of the model, are moved towards the base, the base pressure

increases abruptly at a critical distance. The wake flow is almost cylindrical and for further advance of the obstacle, the base pressure changes relatively little. Evidently the convergent wake flow can become unstable under certain circumstances.

Relatively large quantities of air have been withdrawn from the region of the wake with consequent smooth decrease in base pressure. The addition of moderate amounts of air in the same region gradually increases the pressure.

Except for large objects placed near the model base, the wake flow shows no obvious instability.

3. A Flow Mechanism

We might imagine the base pressure as being determined by the amount of air present in the low velocity region of the wake. Some detailed measurements show that air is being removed along the mixing regions and is being added from the zone of convergence in the wake. Then it might be supposed that the base pressure will be established by a balance of these two factors. As the R. N. decreases, the boundary layer at the model base will increase in size, causing the shearing action of the flow to decrease. Unless this decrease in angle decreases the quantity of air from the convergence zone, the flow would be obviously unstable. Since the base pressure increases smoothly as the R. N. decreases, this stability is present over a fairly wide range of wake angles. The effects of an addition and subtraction on the base pressure are of course consistent with this picture.

Then we shall assume that there is an equilibrium configuration for each Mach number of a parallel stream at the model base.

4. The Two Dimensional Boattail

A square based, two dimensional body is shown in Figure 1.

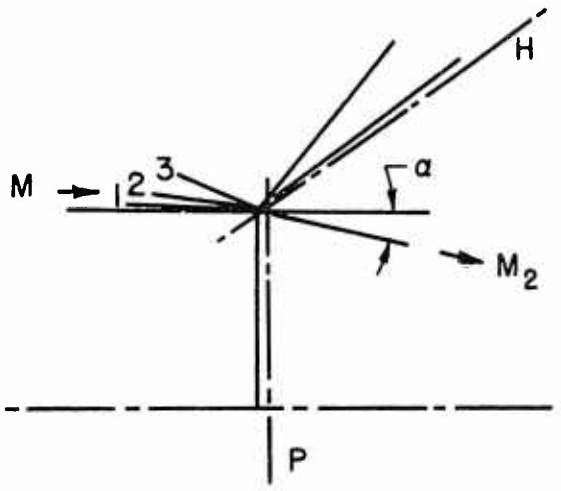

FIG. 1

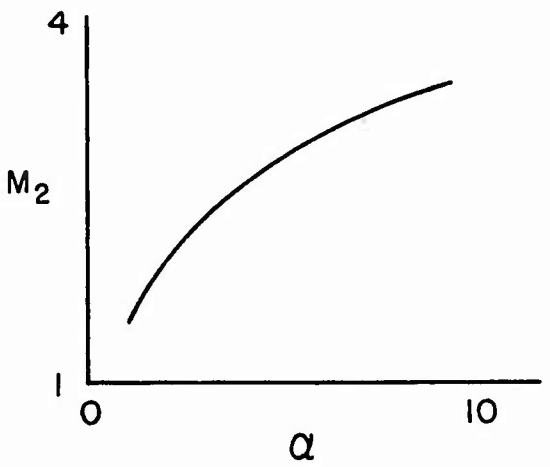

FIG. 2

M_1 is the uniform parallel approach velocity, M_2 and α are the velocity and direction of the air just past the model base. Over a range of M_1s from say $M_1 = 1$ to 4, a function relationship exists between M_2 and α. For bodies of revolution, this function is single valued, and, lacking any evidence to the contrary for 2 dimensional models it is shown accordingly in Figure 2.

Based on the hypothesis of 3, all the flow phenomena involved in establishing the required air balance occurs downstream of planes P and H. Furthermore, for this two-dimensional flow, events upstream of the planes P and H will not affect the flow downstream (Reynold's Number effects have already been discussed). Apparently then, a flow entering the wake at some M_2 and α will adjust M_2 and α until the flow quantities lie on the curve of Figure 2 and consequently the base pressure is unaffected by the boattail angle. In Figure 1, if B. T. 2 slopes at the wake angle, the flow should enter the wake unaltered. B. T. 1 requires an expansion fan at the base and B. T. 3 develops a shock. Clearly, for large angle B. T.s of type 3, a strong shock at the base may affect the boundary layer probably changing the base pressure. Even including the possibility of shock effects, the base pressure should be constant over a significant range of boattail angles.

6. Axially Symmetric Flow in the Wake.

Application of these ideas to flows with axial symmetry encounters prompt difficulties since the Mach Number is no longer a unique function of the boattail angle. The trouble is fundamental and derives from the difference in the source distributions for the two flows. As before, a uniform flow M_1 follows a Prandtl Meyer expansion at the shoulder, but in order to maintain a constant pressure, the angle of the discontinuity surface must increase. In itself, this flow curvature would cause little difficulty, if the curvature for a given M_2 and α, were the same. Unavoidably, the free stream M_1, model shape and conditions obtained at the base affect the shape of the constant pressure region so flows with identical M_2's would enter the convergence zone at different angles producing different pressures.

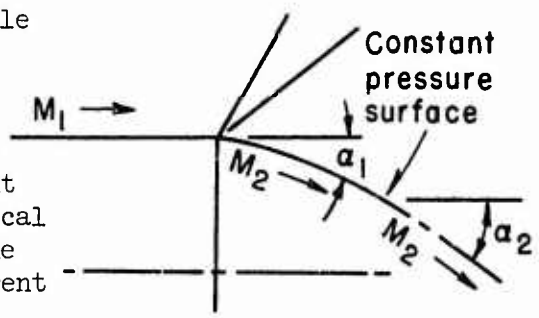

FIG. 3

7. Effect of the boattail (Neglecting the Different Curvature Effect).

Obviously the shape of the boattail for a given approach flow determines its M distribution and it is generally true (at least for convex b.t.) that for any point along the boattail the local M will be lower than if the flow expanded to that local angle from the approach M_1. The parallel flow M which would reach the local M when expanded to the surface angle two-dimensionally will be defined as M_{eff}. Experimentally determined values of the wake angle α, for various $M_{1_{eff}}$s are shown in Figure 4.

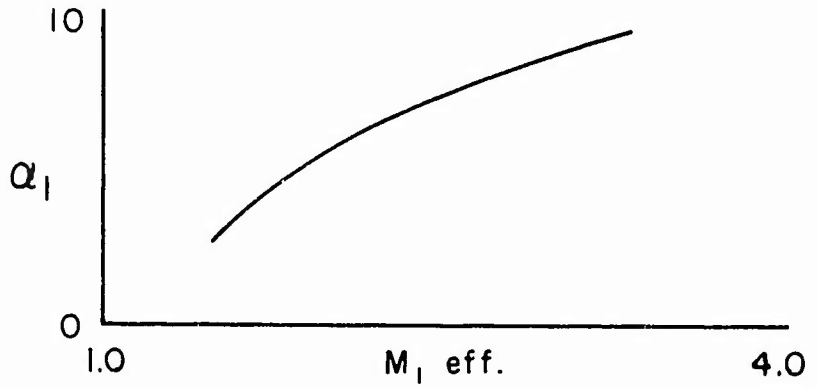

FIG. 4

Neglecting variations in the curvature of the wake bounding streamline is equivalent to assuming that the base pressure will be determined by the local flow conditions at the model base. The local conditions are described in terms of M_{eff} which is taken as the equivalent approach flow so that the base pressure can be rapidly estimated using the static pressure corresponding to M_{eff} and Figure 4.

Suppose we choose a conical b.t. with an angle slightly less than the α_1 for the M_1 at the beginning of the b.t. At the corner the flow will follow a Prandtl-Meyer expansion, but proceeding along the length of the b.t., the M will decrease and the pressure increase. It is clear that if the b.t. is very short, then the surface M will closely approximate the P.M. value at the shoulder and an additional expansion fan will exist at the base. But as the b.t. gets longer, M_{eff} decreases, decreasing α_1 until α_1 equals the b.t. angle. Now the flow enters the wake with no change in direction, while even more extensive b.t.'s should produce base shock waves. Evidently then the drag will decrease as the length of a constant angle b.t. is increased, neglecting skin friction.

Similar considerations can be applied to a boattail with an angle greater than α_1. Again for a very short boattail where the projected area of the b.t. was very small, conditions would be approximately 2 dimensional and the drag would be slightly greater than the square based drag. As the b.t. is lengthened, the surface M decreases, the local pressure increases, and the ratio of base pressure to local pressure increases, so the drag should then decrease as before.

8. The Curvature Effect

Conceivably, under certain circumstances, a difference in wake curvature may be a determining factor, so that even some means of estimating only the order of magnitude of this effect is worthwhile. Again, a discussion of the simpler two dimensional wake first, serves to clarify the concepts involved.

Shock Introduced to Curve Wake

The edge of such a two dimensional wake (upstream of the rise in pressure produced at the convergence zone) would undergo a direction change upon intersection with a superimposed shock (See Figure 5) which reflects from the constant pressure streamline as an expansion wave. The introduction of this shock produces

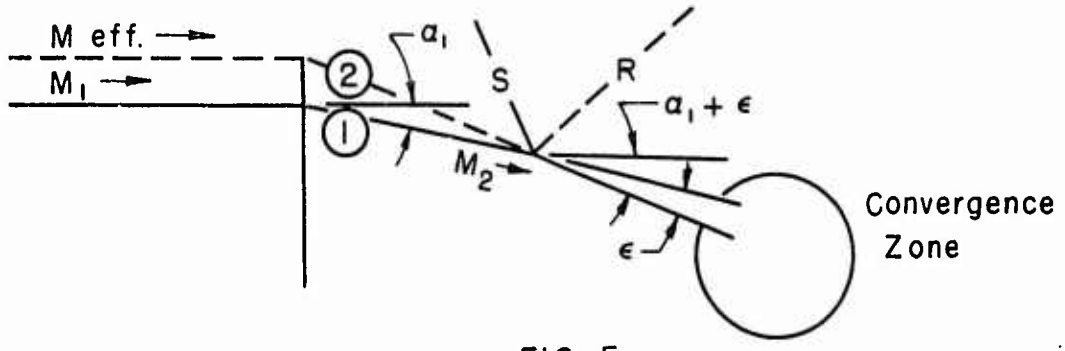

FIG. 5

an altered flow pattern which corresponds to the curved boundary streamline of the axially symmetric flow. Based on the simplified flow model, removal of wake air should be the same with both identical speed along the wake edge and identical length of mixing region. (Since the pressure in the first portion of the wake is sensibly constant, the main flow speed (designated M_2) will remain unchanged after the shock). Now this flow with the shock wave can be compared with a flow without the shock which enters the wake at M_2 and the angle (α +) (after the shock). For convenience, the actual and fictitious flows are designated 1 and 2 respectively. Since the mixing region lengths for both flows are similar, and the angle of convergence is the same, the base pressure should be approximately the same so that flow 2 can be substituted for flow 1. The base pressure will then correspond to the parallel flow M_{eff} required to produce M_2 at (α +) and not to the actual parallel flow M_2. If the shock had intercepted the surface upstream of the base, M_1 would have decreased to M_{eff} thus developing this same base pressure. Different shock position gives same base pressure.

The axially symmetric flow picture is more complicated and does not lend itself to the elementary comparison used in Figure 5 unless numerous assumptions are made. The method described will still represent an attempt to specify a suitable M_{eff} for predicting the base pressure. A typical constant pressure surface for the outer flow of a square based model is shown in Figure 6.

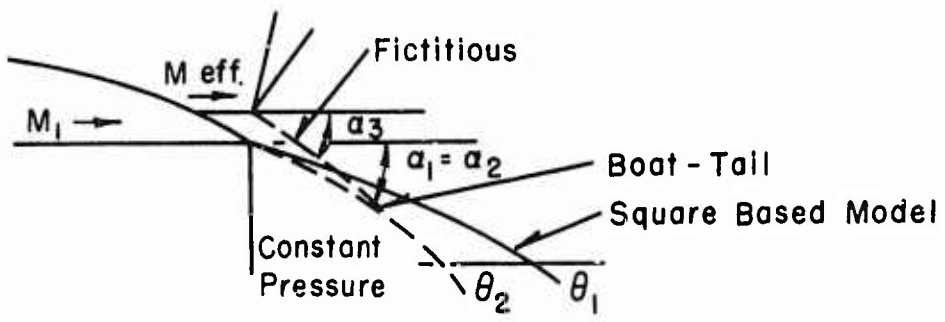

FIG. 6

θ represents the outer flow direction at the end of the constant pressure region of the wake, and, as indicated, it is always larger than α_1, the angle at the model base. The constant pressure streamline (for a b.t. model where M_{eff} (using the method of Paragraph 7) equals M_1 and the flow is required to leave the model base at α_1 (i.e. $\alpha_1 = \alpha_2$) is also shown in Figure 6. It appears most reasonable to assume that the constant pressure region for these two flows ends at the same radius, so that comparing (a) square based model at M_1 and (b) b.t. model with $M_{eff} = M_1$, $\theta = (\theta_1 - \theta_2)$ can be evaluated. A knowledge of $d\theta/d_\alpha$ would permit introduction of a third constant pressure streamline also at M_2 but entering the wake at a modified α_3 so as to produce θ_2 at the final radius. (If necessary, tedious calculations could be made to specify the order of magnitude of $d\theta/d\alpha$). Clearly so specifying α_3, M_{eff} (corrected would be known since the speed along the wake edge is still M_2).

Unclassified
Security Classification

DOCUMENT CONTROL DATA - R&D

(Security classification of title, body of abstract and indexing annotation must be entered when the overall report is classified)

1. ORIGINATING ACTIVITY *(Corporate author)*
U. S. Army Ballistic Research Laboratories
Aberdeen Proving Ground, Maryland

2a REPORT SECURITY CLASSIFICATION
Unclassified

2b GROUP

3. REPORT TITLE
THE EFFECT OF VARIOUS BOATTAIL SHAPES ON BASE PRESSURE AND OTHER AERODYNAMIC CHARACTERISTICS OF A 7-CALIBER LONG BODY OF REVOLUTION AT M = 1.70.

4 DESCRIPTIVE NOTES *(Type of report and inclusive dates)*

5 AUTHOR(S) *(Last name, first name, initial)*
Karpov, Boris G.

6. REPORT DATE	7a TOTAL NO OF PAGES	7b. NO. OF REFS
August 1965	48	7

8a. CONTRACT OR GRANT NO.	9a ORIGINATOR'S REPORT NUMBER(S)
b. PROJECT NO. 1P014501A33D	Report No. 1295
c.	9b. OTHER REPORT NO(S) *(Any other numbers that may be assigned this report)*
d.	

10. AVAILABILITY/LIMITATION NOTICES
Qualified requesters may obtain copies of this report from DDC.
Release or announcement to the public is not authorized.

11. SUPPLEMENTARY NOTES	12. SPONSORING MILITARY ACTIVITY
	U. S. Army Materiel Command Washington, D. C.

13. ABSTRACT

Models, 7 calibers long, with a variety of conical, ogival (convex) and concave boattails were free-flight tested at M = 1.70, for drag and other aerodynamic characteristics. The total drag decreases monotonically for boattails longer than 0.5 calibers. For shorter boattails, the drag is higher than that of the square based body. For boattail lengths between 0.5 and 1.5 calibers, conical boattails have lower drag than either the ogival or concave configurations.

The base pressure decreases with boattail length but increases with the boattail angle at the base.

Among other aerodynamic characteristics, the boattailing appears to cause the most significant change in the Magnus torque coefficient. For certain boattails, this change may be sufficiently large to make the configuration dynamically unstable.

DD FORM 1 JAN 64 1473

Unclassified
Security Classification

14. KEY WORDS	LINK A		LINK B		LINK C	
	ROLE	WT	ROLE	WT	ROLE	WT
Base Pressure Flight Mechanics Aerodynamics of Projectiles						

INSTRUCTIONS

1. ORIGINATING ACTIVITY: Enter the name and address of the contractor, subcontractor, grantee, Department of Defense activity or other organization *(corporate author)* issuing the report.

2a. REPORT SECURITY CLASSIFICATION: Enter the overall security classification of the report. Indicate whether "Restricted Data" is included. Marking is to be in accordance with appropriate security regulations.

2b. GROUP: Automatic downgrading is specified in DoD Directive 5200.10 and Armed Forces Industrial Manual. Enter the group number. Also, when applicable, show that optional markings have been used for Group 3 and Group 4 as authorized.

3. REPORT TITLE: Enter the complete report title in all capital letters. Titles in all cases should be unclassified. If a meaningful title cannot be selected without classification, show title classification in all capitals in parenthesis immediately following the title.

4. DESCRIPTIVE NOTES: If appropriate, enter the type of report, e.g., interim, progress, summary, annual, or final. Give the inclusive dates when a specific reporting period is covered.

5. AUTHOR(S): Enter the name(s) of author(s) as shown on or in the report. Enter last name, first name, middle initial. If military, show rank and branch of service. The name of the principal author is an absolute minimum requirement.

6. REPORT DATE: Enter the date of the report as day, month, year; or month, year. If more than one date appears on the report, use date of publication.

7a. TOTAL NUMBER OF PAGES: The total page count should follow normal pagination procedures, i.e., enter the number of pages containing information.

7b. NUMBER OF REFERENCES: Enter the total number of references cited in the report.

8a. CONTRACT OR GRANT NUMBER: If appropriate, enter the applicable number of the contract or grant under which the report was written.

8b, 8c, & 8d. PROJECT NUMBER: Enter the appropriate military department identification, such as project number, subproject number, system numbers, task number, etc.

9a. ORIGINATOR'S REPORT NUMBER(S): Enter the official report number by which the document will be identified and controlled by the originating activity. This number must be unique to this report.

9b. OTHER REPORT NUMBER(S): If the report has been assigned any other report numbers *(either by the originator or by the sponsor)*, also enter this number(s).

10. AVAILABILITY/LIMITATION NOTICES: Enter any limitations on further dissemination of the report, other than those imposed by security classification, using standard statements such as:

(1) "Qualified requesters may obtain copies of this report from DDC."

(2) "Foreign announcement and dissemination of this report by DDC is not authorized."

(3) "U. S. Government agencies may obtain copies of this report directly from DDC. Other qualified DDC users shall request through _____."

(4) "U. S. military agencies may obtain copies of this report directly from DDC. Other qualified users shall request through _____."

(5) "All distribution of this report is controlled. Qualified DDC users shall request through _____."

If the report has been furnished to the Office of Technical Services, Department of Commerce, for sale to the public, indicate this fact and enter the price, if known.

11. SUPPLEMENTARY NOTES: Use for additional explanatory notes.

12. SPONSORING MILITARY ACTIVITY: Enter the name of the departmental project office or laboratory sponsoring *(paying for)* the research and development. Include address.

13. ABSTRACT: Enter an abstract giving a brief and factual summary of the document indicative of the report, even though it may also appear elsewhere in the body of the technical report. If additional space is required, a continuation sheet shall be attached.

It is highly desirable that the abstract of classified reports be unclassified. Each paragraph of the abstract shall end with an indication of the military security classification of the information in the paragraph, represented as *(TS)*, *(S)*, *(C)*, or *(U)*.

There is no limitation on the length of the abstract. However, the suggested length is from 150 to 225 words.

14. KEY WORDS: Key words are technically meaningful terms or short phrases that characterize a report and may be used as index entries for cataloging the report. Key words must be selected so that no security classification is required. Identifiers, such as equipment model designation, trade name, military project code name, geographic location, may be used as key words but will be followed by an indication of technical context. The assignment of links, rules, and weights is optional.